2010

CELL DEATH AND SUSTAINED SENESCENCE ARREST IN COLON CARCINOMA AND MELANOMA TUMOR CELLS IN RESPONSE TO THE NOVEL MICROTUBULE POISON, JG-03-14

Jonathan Biggers
Virginia Commonwealth University

CELL DEATH AND SUSTAINED SENESCENCE ARREST IN COLON CARCINOMA AND MELANOMA TUMOR CELL RESPONSE TO THE NOVEL MICROTUBULE POISON, JG-03-14

A thesis submitted in partial fulfillment of the requirements for the degree of Master of Science in Pharmacology & Toxicology at Virginia Commonwealth University.

by

Jonathan Biggers,
B.S. Human Nutrition of Foods and Exercise, Virginia Tech

Director: DR. DAVID GEWIRTZ
PROFESSOR, PHARMACOLOGY AND TOXICOLOGY

Virginia Commonwealth University
Richmond, Virginia
July 2010

Acknowledgement

I would like to thank Dr. Gewirtz, the Gewirtz lab, and the entire department for their guidance and much needed assistance. My experience here at VCU has been wonderful and all the support from faculty and students has given me great experiences to keep with me the rest of my life.

I also would like to thank my ever-loving family and friends who have given me much needed support, and kept me driven in times of despair throughout my academic career. Without them I would not be where I am today.

The most thanks to my significant other, Whitney. Without her, I would not have had the strength and perseverance to get through the adversity I have been through the past two years.

Table of Contents

Page

List of Figures

I. HCT-116

II. B16F10

Abstract

CELL DEATH AND SUSTAINED SENESCENCE ARREST IN COLON CARCINOMA AND MELANOMA TUMOR CELLS IN RESPONSE TO THE NOVEL MICROTUBULE POISON, JG-03-14

by

Jonathan Biggers,
B.S. Human Nutrition of Foods and Exercise, Virginia Tech

A thesis submitted in partial fulfillment of the requirements for the degree of Master of Science in Pharmacology & Toxicology at Virginia Commonwealth University.

Virginia Commonwealth University, 2010

Director: DR. DAVID GEWIRTZ
PROFESSOR, PHARMACOLOGY AND TOXICOLOGY

Previous studies from this and other laboratories have shown that the novel microtubule poison, JG-03-14, which binds to the colchicine binding site of tubulin, has the capacity to promote both autophagy and apoptosis in breast tumor cells, as well as interfering with endothelial cell function and potentially disrupting tumor vasculature. The current work was designed to investigate the interaction between JG-03-14 and cell culture models of colon carcinoma and melanoma, specifically HCT116 human colon carcinoma cells and

B16F10 murine melanoma cells. In both cases, JG-03-14 promoted death in the bulk of the treated population. FACS analysis, DAPI and TUNEL staining indicated that only a small fraction of the cell population was undergoing apoptosis; furthermore, there was no evidence of mitotic catastrophe (micronuclei in bi-nucleated cells). Staining with acridine orange and monodansylcadaverine as well as electron microscopy demonstrated the formation of autophagic vesicles, consistent with the cells undergoing extensive autophagy. Cell cycle analysis indicated that cells had arrested in the G2/M stage, with evidence of a hyperdiploid population. Residual surviving cells appeared to be in a state of senescence; furthermore, the senescent cells failed to recover proliferative capacity, indicating that the cells were reproductively dead. Toxicity studies in cardiomyocytes with comparisons to combretastatin and taxol indicated that JG-03-14 was the less toxic of the microtubule poisons. In summary, our studies indicate that JG-03-14 induces autophagic and reproductive cell death in HCT116 colon carcinoma cells and B16F10 murine melanoma cells with limited toxicity to the normal cells that are generally susceptible to taxol and combretastatin. The possibility of alternative mode(s) of cell death (autophagy and irreversible senescence) induced by JG-03-14 makes it a potentially useful candidate as a chemotherapeutic drug that could be used to treat cancers resistant to apoptosis. The relative lack of toxicity of JG-03-14 provides additional support for its potential use in the treatment of malignancies.

CHAPTER 1 Introduction

I. Cancer

Cancer is the second leading cause of death worldwide and is expected to take about 1500 lives per day this year (American Cancer Society, 2010). Two of the more prominent sub-classes of cancer are colorectal cancer, which is the third most prevalent cancer type, and melanoma. Colorectal cancer alone is projected to generate 143,570 cases this year and is estimated to account for 51,370 deaths. In 2009, there were more than a million new cases of skin cancer, including 68,720 cases of the most fatal form, malignant melanoma, with 8,650 deaths associated with melanoma alone (American Cancer Society, 2009).

For both of these cancers, if malignancies are detected early, the tumors can be removed surgically, and the diseases are relatively curable. In contrast, highly aggressive, metastatic lesions of colorectal cancer and melanoma are notoriously resistant to chemotherapy (Fojo et al., 2007; Gray-Schopfer et al., 2007; Gomez et al, 2000), and in cases where these tumors are not detected and removed early in their progression, death is likely to result from the metastatic lesion.

The development of therapies for both metastatic diseases is moving forward quite slowly (Chin et al., 2006; Linos et al., 2009). Colorectal cancer is usually treated with therapies that include 5-fluorouracil, monoclonal antibodies, and inhibitors of EGFR and VEGF (Shia, 2008; Gallegos-Arreola et al, 2008; Zrieki et al, 2008; Schwartz 2008; Igbal and Lenz 2004). Treatment options for late stage melanoma are quite limited and include immunotherapies such as Interleukin-2 and Interferon; however, these have been met with limited success overall (Bajetta et al, 2002). Furthermore, the overall adverse effects of current treatment strategies are quite debilitating and patient side effects such as extreme flu-like symptoms and a host of organ toxicities which need to be closely monitored (Hancock et al, 2004). In order to develop improved approaches for treating these diseases, it is important to identify novel compounds that will be effective at selectively targeting the tumor at pharmacological levels while circumventing common mechanisms of resistance such as decreased accumulation and drug inactivation in tumor cells, increased DNA repair and mutation of drug targets (Eastman and Schulte, 1988; Lai et al, 1988; Cazin et al, 1992).

II. Metastasis and Angiogenesis

As with many cancers, malignant melanoma that has metastasized to distant sites is very difficult to treat and is rarely curable (Hancock et al, 2004; Delaunoit et al., 2005). Melanoma is not only highly metastatic in nature but also is heterogeneous with regards to organ implantation (Kaplan et al., 2005). The

lungs and liver are common organ sites for metastatic disease spread but all organs are susceptible and late relapses are not uncommon (Tsoa et al, 1997). Similarly, colorectal cancer is highly metastatic and most commonly targets the liver. The distant organ lesions for colon cancers yield a 5-year survival rate of only 11% (American Cancer Society, 2010).

The events that lead to the formation of these metastatic lesions may present novel and previously unexplored targets for chemotherapy. It has been found that tumors release tumor specific paracrine and autocrine factors that can trigger bone marrow derived cells and hematopoetic progenitor cell release to alter the micro-environment where the metastatic lesion may implant (Kaplan et al, 2005). In the case of melanoma, this pre-metastatic niche and implantation can occur in any organ, which makes the task of controlling the newly implanted tumors particularly difficult. Cancer cells not only release factors for creating a pre-metastatic niche in distant organs, but also release factors from the bone marrow that will promote the recruitment of endothelial vessels for nutrient supply (Bergers et al, 2003). One of the factors identified as being released by melanoma under hypoxic conditions is vascular endothelial growth factor (Shellman et al, 2003). VEGF is involved with the angiogenic switch which occurs when the tumor is greater than 2 mm in diameter and no longer self sufficient and requires the recruitment and formation of micro-vessels to siphon nutrients from the host (Bergers et al, 2003). Cell division and migration of endothelial cells for generating the tumor blood supply rely on microtubules for function. This indicates that the subunits of microtubules could represent an

ideal target for tumoricidal and tumoristatic cancer chemotherapy, as well as targets for anti-angiogenic prevention of disease recurrence (Pasquier et al., 2008).

III. Microtubules as a Target for Chemotherapy

The cytoskeleton plays a dynamic and intricate role in cell survival and proliferation (Nogales, 2001). Microtubules are a major component of the cytoskeleton and function in transport, mitosis and cytokinesis. In current cancer chemotherapy, a number of drugs target the microtubule subunits in order to effectively disrupt proliferation (Jordan et al, 1998). The drug targets typically bind and sequester the tubulin units, promoting polymerization or bind the established microtubules and depolymerize them (Kuo et al., 2004). Polymerization of microtubules by taxanes and other natural compounds such as the epothilones can lead to arrest in the G2/M phase of the cell cycle followed by apoptosis (Balog et al, 1996; Xiao et al, 2005; Wagenknecht et al, 1998; Blajeski et al, 2001). The microtubule depolymerizing poisons include the vinca alkaloids such as vincristine and vinblastine or the colchicine binding site agents combretastatin A-4, colchicine and 2-methoxyestradiol. The end result of exposure of tumor cells to many of these drugs is effectively an apoptotic response through the induction of cell cycle arrest and effector caspase mediated killing (Moss et al., 2006). However, there is growing recognition of other responses to microtubule poisons including autophagy, aberrant mitosis and senescence (Vicencio et al, 2008; Arthur et al 2007).

IV. Cell Cycle Effects

Microtubule poisons that have been used as chemotherapeutic drugs act through microtubule polymerization or depolymerization; these poisons can also activate cell cycle checkpoints either during the G1 and S phases and/or during spindle assembly. Taxol and other microtubule polymerizers interfere with spindle dynamics and interfere with mitosis (Sudo et al, 2004; Desai, 1997). This spindle disruption can lead to the activation of p53 (Amundson et al, 1998). The role of p53 is complex; p53 will generally arrest cells in G1 through the cdk2-cyclin B inhibitor p21/WAF1/Cip1. There is also evidence that p53 can induce various cell killing pathways including autophagy and apoptosis (Levine et al, 2008; Shen et al, 2001). G1 arrest though is not always permanent and cells can escape the arrest, leading to chromosomal breakage in the subsequent G2 phase (Deckbar et al, 2010). This subsequent chromosomal breakage and slippage may lead to genomic instability and facilitate the development of resistance (Gisselsson, 2001).

Microtubule polymerizers and depolymerizers have strikingly different effects on tubulin subunits but both effectively disrupt cell cycle transitions as cancer therapy (Blajeski et al 2002). Depolymerizers similar to JG-03-14 have been shown to arrest the cell cycle in the G2/M phase, as opposed to the G1 phase observed with many DNA damaging agents and radiation (Ivanov et al, 2007; Zhai et al, 1996; DiLeonardo et al, 2001). Along with the G2/M phase

arrest, some microtubule poisons, including JG-03-14, allow the cell to continually replicate DNA without cytokinesis. This process is called endoreduplication (Moon et al, 2008).

In our studies, we have observed that the G2/M arrest and subsequent generation of a hyperdiploid population is accompanied by autophagic cell death (Arthur et al, 2007). JG-03-14's ability to permanently arrest cells in later stages supports its potential use to promote cell killing and reproductive cell death. G1 arrest, which is commonly short-term arrest, has the potential to produce resistant progeny through the cell re-entering the cell cycle and execution of mitosis (Gisselsson, 2001). The absence of the necessity for apoptosis and possibly the absence of p53 mediated G1 arrest are two potential benefits of utilizing JG-03-14 as a microtubule de-polymerizering agent.

V. Death Responses

A. Apoptosis

The term apoptosis comes from the literal meaning of leaves falling from a tree. Apoptosis is an evolutionarily conserved process where cell death is executed through a family of cysteine-aspartic acid directed proteases knows as the caspase family (Mignotte et al, 1998). In the death receptor extrinsic pathway and intrinsic pathways, the mitochondria release cytochrome c, which is critical to activate apoptotic factors such as Apaf-1 (Scoranno et al. 2003). Cytochrome-c is released from the mitochondria when Bcl-2 family proteins Bax and Bad

homodimerize and form a pore. This pore provides an escape route by which mitochondrial cytochrome c can infiltrate the cytoplasm and form the apaf-1 complex moiety. This Apaf-1 moiety will then form a tetramer called an apoptosome that is capable of cleaving caspase-9 (Twiddy et al, 2007). Caspase-9 is an activator caspase that will cleave caspase-3, which subsequently results in cleavage of poly-ADP ribose polymerase and ultimately destruction of the cell. Apoptotic cell death is characterized by membrane blebbing and the formation of apoptotic bodies, which is accompanied by fragmentation of the nucleus and DNA (Taylor et al, 2008).

Although the apoptotic pathway has been well described, there is mounting evidence that other mechanisms of death may be involved in the response to cancer chemotherapy (Shao et al, 2004; Arthur et al, 2007). In many cases the induction of apoptosis is in response to DNA damage and ultimately leads to cell suicide dependent or independent of p53 (Gulbins et al, 2000). However, tumor cells are notorious for evading apoptotic death through the expression of anti-apoptotic proteins or other mutations (Weinberg, 2000). One common mechanism for evasion of apoptosis is an increase in MDM2, a protein that degrades p53, mutations in p53 or downregulation of p53 (Zhou et al, 2003; Wattel et al, 1994). This is evidence that targeting other modes of cell death would potentially be a useful strategy for cancer chemotherapy.

B. Autophagy

There continues to be controversy in the scientific literature as to whether autophagy is a mode of cell killing or a mode of survival or both. The term autophagy comes from the Greek definition meaning “self eating”. The process is thought to have a multitude of purposes and is activated in response to hypoxic stress or nutrient deprivation (Azad et al, 2008). Nutrient deprivation induced autophagy is thought to be under control of the PI3K-Akt-mTOR pathway (Ravikumar et al, 2004). However, when nutrients are abundant in the presence of chemotherapeutics, the mechanism of autophagic induction is somewhat of an anomaly and yet to be fully described. Regardless, autophagy is initiated by the formation of a double membrane vesicle called a phagophore. This double membrane vesicle can then engulf various cell organelles, specifically damaged mitochondria, peroxisomes or endoplasmic reticulum, forming the autophagosome (Gozuacik and Kimichi, 2004). The autophagosome can then fuse with the lysosome and digest the organelles to basic amino acids and theoretically provide energy. This process is controversial because the recycling of degraded products may be aiding in survival, or approach a critical threshold and result in cell death (Alva et al, 2004).

This autophagic response has been observed in response to a growing number of investigative chemotherapy agents. (Arthur et al, 2007; Cui et al, 2007). The development of resistance to apoptotic machinery and specifically the general lack of sensitivity to chemotherapy of metastatic cancers contribute to the potential utility of autophagic cell death (programmed cell death II) as a target for novel chemotherapeutic agents. Metastatic disease is notoriously

resistant to common therapies and the possibility of exploiting autophagy as a primary mechanism of cell killing could be beneficial.

After the initial disruption and cell killing, the cells may also be forced into a state of reproductive death where they still metabolize but are no longer replicating (Weaver et al, 2005; Vicencio et al., 2008). It has also been shown that senescent cells release cytokines that can promote removal via the immune system (Bartek et al., 2008; Xue et al., 2007). In a similar fashion, autophagic cells may have a component to trigger activation and clearance by the innate immune system (Thornburn et al., 2009).

C. Mitotic Catastrophe

Mitotic catastrophe has long been recognized as a mode of cell death, but understanding the mechanisms that promote mitotic catastrophe has posed a long-standing challenge (Castedo et al, 2004). The current understanding is that mitotic catastrophe is cell death resulting from aberrant mitosis as a consequence of deficient cell cycle checkpoints (Vakifahmetoglu et al., 2008). The cells prematurely enter into mitosis and the attempt of the cellular machinery to separate aberrant chromosomes may result in the formation of micronuclei and nuclear fragments (Erenpreisa et al, 2001). Cells which undergo mitotic catastrophe slip past cell cycle checkpoints leading to arrest in late stages of cell cycle (Vakifahmetoglu et al, 2008). This study also mentions that mitotic catastrophe may be a pre-stage for apoptosis. The JG-03-14 compound has not been shown to promote the formation of micronuclei and the treated cells do not

appear to contain bifurcated nuclei (Arthur et al, 2007). This mechanism of cell death remains ambiguous and requires further understanding before it can be exploited in chemotherapeutic investigations.

VI. Senescence

The term replicative senescence refers to the inability of a cell to divide indefinitely (Campisi et al., 2007). Most cancer cells have an enzyme called telomerase that creates an extension of the telomeric DNA with each division and allows for immortality and unlimited proliferation (Campisi, 1997). Studies have also shown that cancer cells will respond to chemotherapy with a similar form of reproductive death, termed accelerated senescence (Di et al, 2009). Accelerated senescence can occur in response to DNA damage induced by radiation or chemotherapy. A recent commentary described how, in response to chemotherapeutic agents, cells can activate the ATM/ATR pathways which will phosphorylate chk1/chk2 (Gewirtz et al., 2008). This phosphorylation will have multiple downstream effects including the phosphorylation and activation of p53. The phosphorylation of p53 has also been shown to activate p21, which can inhibit cyclin dependent kinases. Cyclin dependent kinase inhibition leads to activation of the Rb protein through dephosphorylation. This dephosphorylation permits Rb to interact with E2F and promote this accelerated senescence (Di et al, 2009; Gewirtz et al, 2008). This arrest theoretically will allow time for the cell to repair DNA in to avoid passing the damaged DNA to daughter cells (DiLeonardo, 1994). The induction of accelerated senescence and pathway

description is with regards to DNA damaging agents such as topoisomerase poisons and ionizing radiation (Di et al, 2009).

The JG-03-14 compound has been shown to induce senescence in p53 wild-type MCF-7 cells but not the mutant p53 MDA-MB-231 (Arthur et al, 2007). This senescent response appears to occur in the residual cells and not as the primary mechanism of action. The growing intimacy between autophagy and senescence may indicate that JG-03-14 induces autophagy and cells either die or enter into a state of senescence (Arthur et al., 2007; Narita et al., 2009; Vicencio et al, 2008). This may implicate autophagic cell death as a bridge in residual cells to undergo senescence possibly through the generation of reactive oxygen species (Di et al, 2009). Adding to the intimacy between these pathways, the inhibition of autophagy or sequestration of reactive oxygen species have been shown to attenuate senescence and in some cases increase the amount of apoptotic cell death (Young et al, 2010; Di et al, 2009).

VII. The Conjugated Pyrrole, JG-03-14

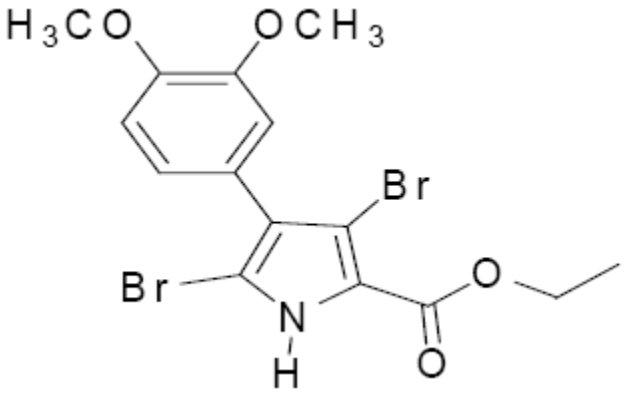

The compound currently under investigation is a di-brominated conjugated pyrrole, which has shown cell-killing effects in multiple cell cancer cell lines (Arthur et al, 2007; Mooberry et al, 2007; Nguyen, MS Thesis). Pyrroles are components of more complex macrolides that contain multiple aromatic rings (Juselius et al, 2000). These pyrrole compounds and analogs such as imidazoles and lamellarins are widely being investigated as pre-clinical anti-cancer therapies (Bright et al, 2010; Iguchi et al, 2002; Baunbæk et al, 2008). Early investigations have found that the JG-03-14 and its analogs bind to the colchicine-binding site of tubulin and have depolymerizing effects on microtubules (Mooberry et al, 2007). This latter study also demonstrated that JG-03-14 has similar efficacy in competitive binding assays to Combretastatin A-4 and [H-3] colchicine. JG-03-14 has also been shown to be effective at killing MCF-7, MCF-7/E6, and MDA-MB-231 and 4T-1 metastatic breast tumor cells, HCT-116 colon carcinoma cells, and B16F10 melanoma cells through both autophagy and apoptosis possibly independent of p53/p21 induction (Arthur et al, 2007; Mooberry et al, 2007; this thesis). These cell lines include both p53 wild type such as MCF-7 cell lines, HCT-116 cell line and B16F10 cell line. The MDA-MB231 is of the p53 mutant genotype.

In addition to direct antitumor effects, JG-03-14 has been reported to prevent, as well as disrupt existing endothelial vessel formation (Daylot-Herman et al, 2009). The concentrations of JG-03-14 determined to inhibit endothelial function were found to be sub-toxic in comparison to colchicines and nocadozole which required concentrations high enough to induce apoptosis of the endothelial

cells (Daylot-Herman et al, 2009). Colchicine cannot be used clinically because it is extremely toxic to patients and is also a substrate for the p-glycoprotein pump (Druley et al, 2001; Mooberry et al, 2007). Our compound of interest, JG-03-14, is not a substrate for the multi drug resistance P-glycoprotein pump, which should be a decided advantage over other compounds of the same class (Mooberry et al, 2007).

Considering the demonstrated need for effective therapies against metastatic colon cancer and the high propensity for melanoma to metastasize, we evaluated whether this compound would be effective against tumor cell lines derived from these malignancies. Our aim with this series of studies was to further enhance the understanding of the JG-03-14 compound with regards to apoptosis, autophagy and senescence. To prove that autophagy is acting as a primary mechanism of cell killing and show that apoptosis and senescence are intimately linked to the process. Another goal was to expand on the effects of this microtubule poison in a variety of cell lines and investigate the advantages of an anti-angiogenic conjugated pyrrole as a potential chemotherapeutic drug.

CHAPTER 2 Methods and Materials

Cell Culture HCT116 colon carcinoma cells were obtained from ATCC and kept frozen in 10% DMSO (Sigma Chemical, St. Louis, MO) with Fetal Bovine Serum (FBS) (GIBCO Life Technologies, Gaithersburg, MD) until use. HCT-116 cells are quickly thawed and cultured in a T75 flask (Cellstar) in basal RPMI 1640 medium supplemented with 5% fetal bovine serum, 5% bovine calf serum, 2 mM L-glutamine, and penicillin/streptomycin 0.5 ml/100 ml medium (10,000units/ml penicillin and 10 mg/ml streptomycin, GIBCO Life Technologies, Gaithersburg, MD) at 37° C under a humidified, 5% CO_2 atmosphere. B16F10 murine melanoma cells were generously provided by Dr. Kimber White from ATCC and kept frozen and harvested the same as described for HCT-116. B16F10 cells were cultured in RPMI 1640 medium supplemented with 10% fetal bovine serum, 2 mM L-glutamine, penicillin/streptomycin 0.5/100 mL (10,000 units/ml penicillin and 10 mg/ml streptomycin), 1M HEPES and 7.5% NaBicarbonate (GIBCO Life Technologies, Gaithersburg, MD and Sigma-Aldrich). H9c2 rat embryonic cardiomyocytes were thawed and plated as described above. H9c2 cells were maintained in culture with DMEM medium supplemented with 10% fetal bovine serum, and streptomycin/penicillin as described above.

All Cells were passaged at 80% confluency by washing one time with 1X PBS(GIBCO) and harvested with trypsin-EDTA 0.25 %(GIBCO) then deactivated with RPMI medium, collected and centrifuged at 15,000 rpm for 3 minutes. Medium was aspirated and fresh media is added to the cell pellet; cells were resuspended in media and 300 µL of the cell resuspension was placed into a fresh T75 flask with 10mL RPMI medium. For all culture experiments, cells were plated and permitted to adhere overnight before drug treatment. Unless otherwise indicated, all treatment involved continuous drug exposure.

MTT assay 5,000 cells in150µL media were plated in each well of a 96 well dish and allowed to adhere overnight before drug treatment. After 48 hours, 100 µL of the MTT solution (2mg/mL PBS prepared in the dark) was added to each well and incubated for 3 hours at 37° C The MTT solution was removed, 100µL of DMSO was added to each well, and the blue dye was allowed to dissolve for 5 minutes. An absorbance reading was taken at 490 nm (KC Junior software, EL800 Universal Microplate Reader).

Time Course of Drug Effects on Viable Cell Number and Proliferative Recovery Cells were plated at $1x10^6$ cells per 96 mm Petri plate (CellStar) and allowed to adhere overnight. At the various time points, the drug was aspirated and cells were washed once using 1X PBS. Cells were then harvested and

centrifuged at 15,000 rpm for 3 minutes and media was removed. The cell pellet was resuspended in fresh media and 10μL of the cell resuspension was added to 90μL of trypan blue exclusion dye (1:9; trypan blue: PBS). 10μL of the mixture was placed onto a hemocytometer and viable cells (those that excluded the dye) were counted in 4 separate quadrants (each quadrant containing 16 squares).

DAPI Staining Hoechst dye for Apoptosis and Mitotic Catastrophe At the various time points, both adherent and non-adherent cells were harvested and centrifuged at 15,000 rpm for 3 minutes. The media was aspirated and fresh media was added to resuspend the pellet. Cell number was determined using trypan blue exclusion. A dilution of 20,000 cells in 200 μL of 1X PBS per slide were prepared and cells were spun at 10,000 rpm for 5 minutes (Shandon Cytospin 4, Thermal Electron Corp). Slides were refrigerated until ready for staining. Cells were fixed with 4% formaldehyde in PBS for 10 minutes at room temperature, and then washed with PBS twice for 5 minutes at room temperature. A 1:2 dilution of acetic acid and ethanol was used to fix the cells at 20° C for 5 minutes. The slides were then washed twice with PBS for 5 minutes at room temperature. A 1:1000 dilution was prepared for Vectashield :Dapi and each slide was mounted with 10μL of the solution. Coverslips were sealed using clear nail polish and photographs were taken with a 10X objective lens using a Nikon fluorescence microscope and an Olympus camera. Slides were stored at 4°C , and three fields per condition were evaluated.

Both adherent cells and supernatant were collected at various time points and centrifuged at 1200 rpm for 5 min at 5°C. Cells were then resuspended in 5 mL of PBS and centrifuged again. Supernatant from the centrifuge was aspirated and cells were then resuspended in 0.075 M KCl by finger tapping and allowed to incubate for 8 minutes at room temperature. Cells were again centrifuged and supernatent was aspirated. Cells were then fixed in the pellet with a 3:1 ratio of methanol and glacial acetic acid. Samples were then dispersed on a slides moisturized with deionized water. Slides were stored overnight to dry. To stain the cells, Hoechst dye was diluted to 1:500 dilution of 1 mM Hoechst 33342 in nanopure water for 10 minutes at room temperature. The slides were then rinsed once and sealed similar to slides for DAPI.

TUNEL staining for apoptosis

The method of Gavrieli et al. was utilized as an independent assessment of apoptotic cell death in combined cytospins containing both adherent and non-adherant cells, as reported previously (Elmore et al., 2002; DeMasters et al., 2006). Cells were fixed and fragmented DNA in cells undergoing apoptosis were detected using the In Situ Cell Death Detection Kit (Roche), where strand breaks are end labeled with fluorescein dUTP by the enzyme terminal transferase.

Flow Cytometry Cells were plated at 3x 10^6 million cells per 96 mm Petri plates for each time point and allowed to adhere overnight. Setup was prepared for day

5 and worked backward so that all treatments would complete on the same date. Drug treatment was initiated the following day and drug was left on the cells for continuous exposure. Upon the completion of treatment, media was aspirated and cells were washed one time with 1X PBS. Cells were harvested using trypsin and deactivated with 10ml media, then centrifuged at 15,000 rpm for 3 minutes. Media was aspirated and the cell pellet was resuspended in fresh media. Cell numbers were determined using trypan blue exclusion dye. At least $1x10^{6}$ cells per condition were used in the cell cycle analysis. 1.5 mL of Propidium iodide stain with RNAse was added to each aliquot of $1x10^{6}$ cells. The cell suspension was filtered through a 70 micron mesh 2 times. All samples were covered in aluminum foil and refrigerated until the next day. FACs acquisition was performed using the EPICS 753 flow cytometer (Coulter Electronics, Hialeah, FL) using a 488 nm argon laser and standard optical emission filters. A minimum of 13,000 events were collected per sample. Cellular DNA distributions were analyzed at the various stages of the cell cycle using Cytologic Software (Coulter Electronics).

Acridine Orange and Monodansylcadaverine staining for autophagy As a marker for autophagy, the acridine orange staining method described by Paglin et al, 2001 was used. Cells were plated at 2×10^{5} per 6 well plate and allowed to adhere overnight. Drug was added the following day and left on for continuous exposure. At the final time point, the drug was removed and cells were washed one time with 1X PBS. Cells were then stained with acridine orange (1ug/ml) for

15 minutes. Monodansylcadaverine(MDC) is another marker for autophagy that stains the autophagic membrane (Niemann et al, 2000). MDC(Sigma) was dissolved in DMSO and diluted to 0.1 mM. At selected time points, cells were stained with 0.1 mM monodansylcadaverine for 10 minutes. The stain was removed and cells were washed with 1X PBS four times before fresh media was added to the wells. Pictures were taken with the inverted Nikon fluorescence microscope and an Olympus camera with 20X objective lens.

Transfection with RFP-LC3 HCT-116 HCT-116 cells were prepared from frozen stock and passaged twice at least 2 days before nucleofection. $1x10^6$ cells were centrifuged and suspended in a pellet. 100 µL of the Nucleofector V (Nucleofector Kit V, Amaxa) mix was added to to resuspend the cells. The resuspension was added to 1 µg of the RFP-LC3 vector and the entire suspension was transferred to the cuvette. The cuvette was placed in the Nucleofector device and program D-032 was used to transfect the cells. 500 µl warm medium was added to the transfected solution and the total suspension was transferred to a Petri plate. These steps were repeated for the positive and negative controls using 2 µg of empty-GFP, and 2 µg pmax-RFP. Stable transfection was maintained using Gentimycin at 1µg/125 mL.

Electron Microscopy Cells were harvested from culture and $1x10^5$ cells were plated per plate on Permanox Petri dishes. Various drug treatments were performed until endpoint. At each time point, cells were washed with 1X PBS

and then fixed with 2% paraformaldehyde/2 % glutaraldehyde in 0.1M sodium cacodylate buffer. After 1 hour at room temperature, fixative was removed and replaced with 0.1M sodium cacodylate buffer, pH 7.4. Plates were then fixed in 1% osmium tetroxide in 0.1M-cacodylate buffer for one hour, after which they were rinsed in 0.1M cacodylate buffer for 5-10 minutes. The plates were then dehydrated in graded ethanol series: 50%, 70%, 80%, 95%; for 5-10 minutes each. Then cell plates were dehydrated in 100% ethanol 3X, 10-15 minutes each. This was followed by propylene oxide 3X, 10–15 minutes each. Cells were then infiltrated with 50/50 mix of propylene oxide and PolyBed 812 resin mix overnight. Next, the cells were infiltrated with pure PolyBed 812 resin (Polysciences, Inc.) mix hours and overnight. The cells were placed in embedding containing PolyBed 812 and placed in 60˚C oven overnight to polymerize. Sectioning was done using Leica EM UC6i Ultramicrotome (Leica Microsystems). Semi-thin sections for light microscopy (0.5µm – 1.0µm) were collected on glass microscope slides and stained with 0.1% toluidine blue/0.1% azure II/0.1% methylene blue in 1.0% sodium borate. For electron microscopy, 70-90 nm thick sections were collected on copper mesh grids and stained with 5% uranyl acetate and Reynold's lead citrate. Images were taken using JEOL JEM-1230 TEM (JEOL USA, Inc.) with the Gatan Ultrascan 4000 digital camera (Gatan Inc, Pleasanton, CA).

Western Blotting After the indicated times, cellular proteins were extracted from treated cells $1x10^6$ using 100 to 200 µL of 1X Tris lysis buffer (1 M Tris(pH 6.8),

10% SDS, and dH2O) containing protease inhibitors with boiling for 5 minutes. Protein concentration was determined with a Lowry protein assay and 10 µg of total cell lysates were separated using 12% SDS-PAGE. Proteins were transferred onto nitrocellulose membrane for 1 hour and blocked in TBS-Tween 20 buffer containing 5% nonfat dry milk. Membranes were then immunoblotted with the respective primary antibodies overnight in 20°C. The following day, the membrane was incubated with horseradish peroxidase-conjugated secondary antibody for 1 hour. Signals were detected using an enhanced chemilluminescence detection reagents from Pierce (Rockford, IL).

Beta-galactosidase Staining for Senescence Senescence was determined based on β-galactosidase staining in the HCT-116 after exposure to indicated drug treatments. Cells were washed twice with PBS and fixed with 2% formaldehyde, 0.2% glutaraldehyde for 5 min. The cells were washed again with PBS and stained with a solution of 1 mg/mL 5-bromo-4-chloro-3-inolyl-β-galactosidase in dimethylformamide (20 mg/mL stock), 5 mM potassium ferrocyanide, 5 mM potassium ferricyanide, 150 mM NaCl, 40 mM citric acid/sodium phosphate, pH 6.0, and 2 mM $MgCl_2$. Following overnight incubation at 37 °C, the cells were washed twice with PBS and the images were capture for visualization.

Clonogenic Survival Clonogenicity were determined with 72 hours of drug treatment followed by washing of cells and replacement with fresh media. Plates

were washed 1x with PBS prior to fixation with 100% methanol for 10 minutes. After removal of methanol, plates were stained with crystal violet dye (1%) in deionized water for 10 minutes. Colonies were based on visual staining. Vehicle treated, JG-03-14 10nM and 100nM all received 500 cells while JG-03-14 250nM and 500nM receive 2500 cells. Treatment groups were corrected for plating efficiency.

DCF Staining for Reactive Oxygen Species

Cells were plated in 6-well plates at a density of $5x10^4$ per well. After treatment cells were incubated with 50 μM non-fluorescent DCF and intracellular reactive oxygen species were visualized when di-acetate group are hydrolyzed to fluorescent 2', 7'dichlorofluorescein upon interaction with reactive oxygen species. Images were taken using the same methodology as acridine orange and MDC.

Statistical Analysis

Statistical analysis was performed using the Statview computer software. ANOVA testing was performed and post-hoc analysis determined significance base on a p-value of $P<0.05$.

CHAPTER 3 Results

Part I. Effects of JG-03-14 on HCT-116 colon carcinoma cells

I. Growth inhibition of HCT-116 colon cancer cells by JG-03-14.

Initial studies evaluated the sensitivity of HCT-116 colon carcinoma cells to JG-03-14 using the MTT dye assay (Mosmann, 1983). Cells were exposed to JG-03-14 continuously for 48 hours prior to assessment of viable cell number. JG-03-14 was ineffective at a concentration of 100nM, but produced > 50% growth inhibition at 250nM, and > 70% inhibition at 500nM (Figure 1), findings similar to what were reported previously in breast tumor cells (Arthur, 2007). All subsequent studies were performed using JG-03-14 at a concentration of either 250nM or 500 nM. Sensitivity to Combretastatin A-4 was intended as a positive control.

Cells were also assessed for clonogenic capacity after the initial 72 hours treatment. Cell number was corrected for plating efficiency and calculated as a percent of control. Table 1 indicates that treatments of HCT-116 cells with JG-03-14 at concentrations of 250 nM and 500 nM showed loss of colony forming capacity of 95% and 98%, respectively (Table I).

II. Cell death induced by JG-03-14.

In order to distinguish between the effects of JG-03-14 on cell growth and on overall viability, we monitored cell viability by trypan blue exclusion in cells continuously exposed to JG-03-14 over a period of 5 days. Figure 2 shows a time dependent decline in the number of viable HCT-116 cells upon continuous exposure to JG-03-14 at 500nM, a concentration that was previously found to be effective in promoting breast tumor growth arrest and cell death (Arthur, 2007). The figure inset clearly demonstrates that the tumor cells exposed to JG-03-14 were dying, with approximately 95% of the HCT-116 cells lost after a period of 3 days.

III. Assessment of the mode of cell death

In previous studies, we have reported that JG-03-14 promotes primarily autophagy in p53 wild type MCF-7 cells and both autophagy and apoptosis in p53 mutant MDA-MB231 cells (Arthur, 2007). As HCT-116 cells are wild type in p53, it was our expectation that cell death might also occur primarily via autophagy. Nevertheless, we also examined the possibility of both apoptosis and mitotic catastrophe in response to treatment with JG-03-14. Apoptosis was assessed based on nuclear fragmentation by Hoechst, DAPI and TUNEL staining. Autophagy was evaluated based on acridine orange and monodansylcadaverine staining, electron microscopy as well as redistribution of RFP-LC3 and autophagic flux using p62. Mitotic catastrophe was based on the

formation of bi-nucleated cells with micronuclei (DeMasters et al, 2006). Figure 3 shows the untreated vehicle control with a clearly defined intact nucleus. With a few isolated exceptions, the nuclei of cells treated with JG-03-14 were intact although significantly enlarged in comparison to control cells, with little evidence for either apoptosis (Figure 3A) or mitotic catastrophe using a higher magnification with Hoechst (Figure 3B). The absence of apoptosis was also confirmed by absence of TUNEL positive staining (Figure 7C) and supported by FACS analyses performed previously by Tuyen Nguyen (MS Thesis, 2008). In contrast, taxol promoted extensive nuclear fragmentation, indicative of apoptosis while combretastatin treatment resulted in mitotic catastrophe (Bartek & Lukas, 2001).

Previous work by Ms. Nguyen also indicates that JG-03-14 transiently arrested 66.4% of the HCT-116 p53 wild type tumor cells in the G2/M cell phase after the first day of treatment. This G2/M block persisted for at least 72 hours. After 72 hours, the cell cycle distribution shifted, with 63% of the cells in G2/M and 4.5% in G1, with a very small sub G1 population. Of particular interest was the observation that these p53 wild type cells appear to continue to replicate their DNA following the G2/M arrest, resulting in a hyper diploid population. This effect was observed after the first day of treatment and the hyper diploid cell population had more than doubled after 72 hours. In contrast, Taxol arrested 41.72% of cells in the G1/G0 phase after just 24 hours, and this cell cycle distribution grew to 59.76% after 72 hours.

In summary, only a small fraction of the cell population could be detected in the sub G1 phase both at 24 and 72 hours following the initiation of treatment with 500 nM JG-03-14, confirming that apoptosis likely plays only a minor role in cell death induced by JG-03-14 in the HCT-116 cells.

In contrast to the relative lack of apoptosis, there was extensive evidence of autophagy after treatment with JG-03-14 in the HCT-116 cells. Figure 4A shows that control HCT-116 controls stained with acridine orange had a single large vesicle that was situated near the nucleus; in contrast, extensive punctuate distribution of small acidic vesicles within the cytoplasm, indicative of autophagy, was observed in cells treated with JG-03-14. The cells treated with JG-03-14 were also quite enlarged, nearly double the size of the untreated cells.

Utilizing monodansylcadaverine, a stain that binds to the lipid membrane of the autophagosomes, results in similar patterns to what was observed with the acridine orange staining. Specifically, as shown in figure 4B, the controls show a single vacuole closely associated with the cell nucleus while the cells treated with JG-03-14 show a highly distributed punctuate pattern throughout the cytoplasm.

LC3-II is a cleaved product of LC3-I and is involved in the formation of autophagosomes (Kabeya et al, 2000). We further monitored the distribution of LC-3 II in the treated cells. HCT-116 colon tumor cells were transfected with an RFP-LC3 vector via nucleofection and the cells were observed under fluorescence after 72 hours of exposure to 500 nM JG-03-14. After 72 hours of

drug treatment, the transfected cells showed a punctuate distribution of LC-3 II proteins in the cytoplasm, again consistent with the promotion of autophagy (Figure 5A).

In order to further confirm autophagic flux, we monitored p62 protein expression. This is a scaffold protein associated with autophagic membrane formation. The flux and degradation of p62 indicates that the autophagic machinery is in effect degrading the membrane to completion (Bjørkøy et al, 2009). In HCT-116 cells treated with 500 nM JG-03-14 for 48 hours, we observed a clear reduction in p62 protein expression. This reduction was also inhibited with a late stage autophagic inhibitor, Chloroquine (Figure 5C). Starvation was included as a positive control for degradation of p62.

Another method to visualize autophagic vesicle formation is the use of electron microscopy imaging (Ylä-Anttila, et al., 2009). This is a gold standard for vesicle formation. The image in figure 5B clearly shows the induction of autophagic vesicles after 72 hours of treatment with 500 nM JG-03-14.

IV. Effect of autophagic inhibition on JG-03-14 induced cyto toxicity

The role of autophagy is still undefined and appears to have a role in both cell protection and cell killing. In efforts to confirm that JG-03-14 is killing the HCT-116 cells through autophagic processes, studies assessed the impact of inhibition of autophagy on tumor cell sensitivity to JG-03-14. As shown in figure 6A, the concurrent treatment of cells with JG-03-14 and chloroquine was only slightly protective. Chloroquine is a lysomotropic inhibitor, which merely

maintains pH and prevents acidification of autophagic vesicles, only preventing the last step of autophagy (Shintani et al., 2001). In figure 6B, it is clear that chloroquine produces a blockade to autophagy, as shown by condensed fluorescent staining. More quantitative evidence that chloroquine blocks autophagic flux is provided by figure 5B, which shows that concurrent treatment with JG-03-14 and chloroquine protected p62 from degradation.

The fact that inhibition of autophagy did not provide complete protection to the cells suggested that a blockade to autophagy was likely to be leading to an alternative mode of cell death, specifically apoptosis. Figure 6C clearly shows a large increase in TUNEL positive staining for concurrent treatment with JG-03-14 and chloroquine. Combretastatin A-4 is utilized as a positive control for induction of apoptosis.

V. Promotion of senescence and lack of proliferative recovery in residual surviving cells

In previous studies, we have reported that residual cells that appear to have survived the drug treatment were in a state of senescence arrest (Arthur, 2007); in some reports, senescence has been succeeded by proliferative recovery (Sliwinska, 2009; Elmore et al., 2005). In the current studies, we observed that the residual cell population that survives the initial cytotoxic effects of JG-03-14 is arrested in state of senescence, based on beta-galactosidase staining as well as cell enlargement and spreading (Figure 7A). Three days post treatment, nearly

100% of the residual surviving population stained positively for beta galactosidase (Figure 7B).

Although senescence is generally thought to be irreversible, we have observed recovery of proliferative capacity in breast tumor cells subsequent to treatment with either doxorubicin or radiation (Sliwinska, 2009; DeMasters, 2004; Jones et al., 2005). In order to determine whether the cells exposed to JG-03-14 had lost self-renewal capacity, drug was removed after 3 days, and cell number was followed for an additional 17 days. However, we failed to detect any evidence of re-growth, indicating that the cells had apparently lost all reproductive capacity (Figure 7C).

VI. Reactive Oxygen Generation as Possible Role in Toxicity

The studies in Figure 8 compared reactive oxygen generation by JG-03-14, taxol, and combretastatin by DCF staining generated significantly less reactive oxygen after 72 hours than the other compounds (Figure 8). This reactive oxygen generation likely contributes to the toxicity generated by these clinical therapeutic agents, specifically cardiotoxicity and peripheral neuropathy (Kim et al, 2004).

Table 1 – Clonogenic Survival following exposure with JG-03-14 (% control)	
250 nM	**500 nM**
4.65 ± 0.07*	1.65 ± 0.25*
Values represent average colonies formed 2 weeks post 72 hours treatment with JG-03-14 * P= <0.0001 compared to Control group	

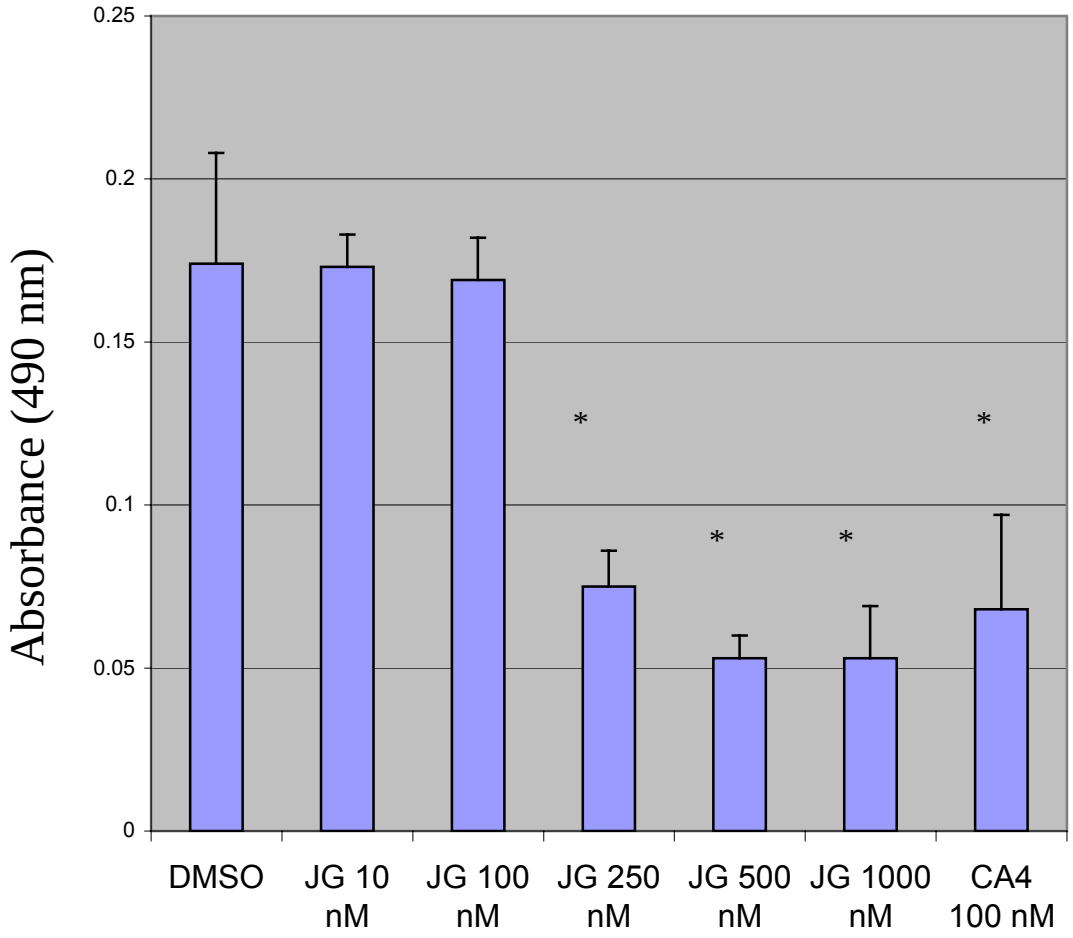

Figure 1. Sensitivity to JG-03-14 in HCT-116 cells. Cells were exposed to JG-03-14 at the indicated concentrations for 48 hours and cell number was evaluated using the MTT dye assay. Values shown are from a representative experiment with quadruplicate samples for each condition. Studies were reproduced in 3 additional replicate experiments. Error bars reflect standard deviations and significant differences from DMSO treatment are indicated by * ($P<0.05$), which were assessed by the ANOVA and Tukey/Kramer post-hoc analysis.

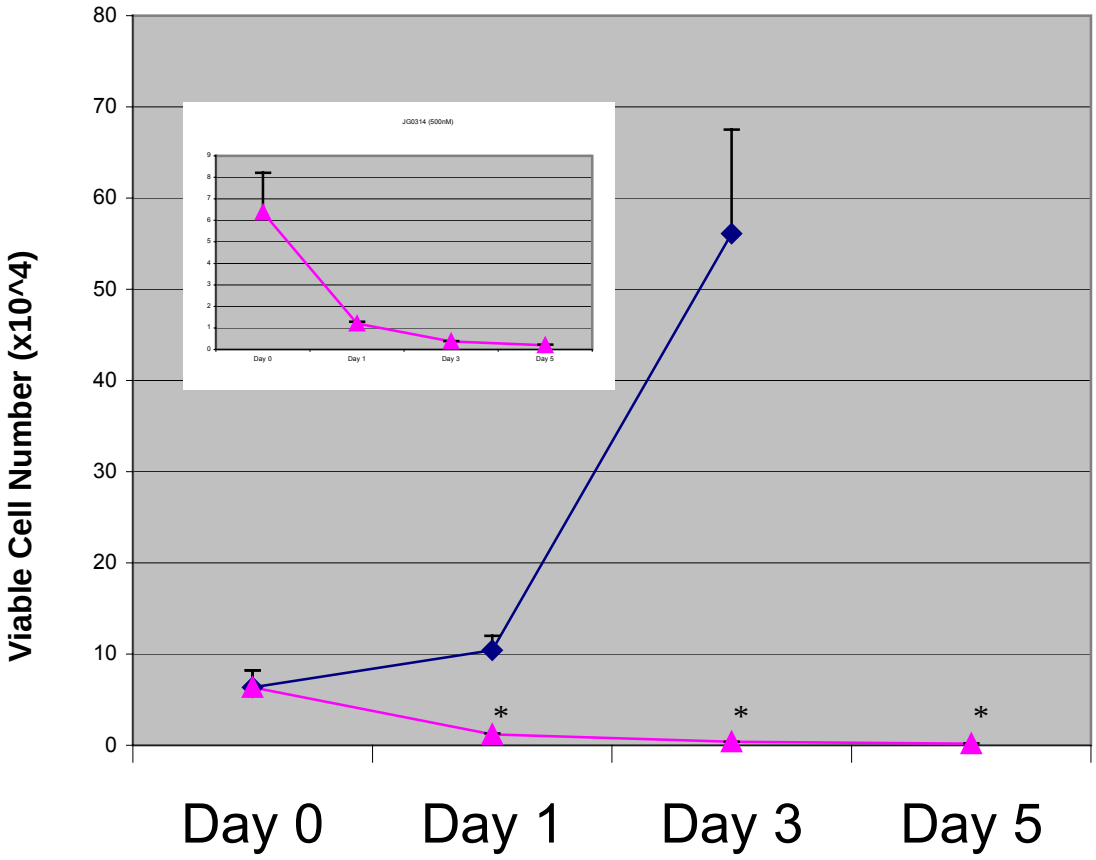

Figure 2. Time dependent loss in cell viability by exposure to JG-03-14. HCT-116 cells were either continuously exposed to DMSO or 500nM JG-03-14 and viable cell number was monitored by trypan blue exclusion over a period of 5 days. Values shown are from a representative experiment with triplicate samples for each condition. Studies were reproduced in 3 additional replicate experiments. The inset shows the decline in viable cell number using an expanded Y-axis. Significance differences from DMSO treatment are indicated by * ($P<0.05$) and were assessed by ANOVA and Fisher's PLSD post-hoc analysis.

A.

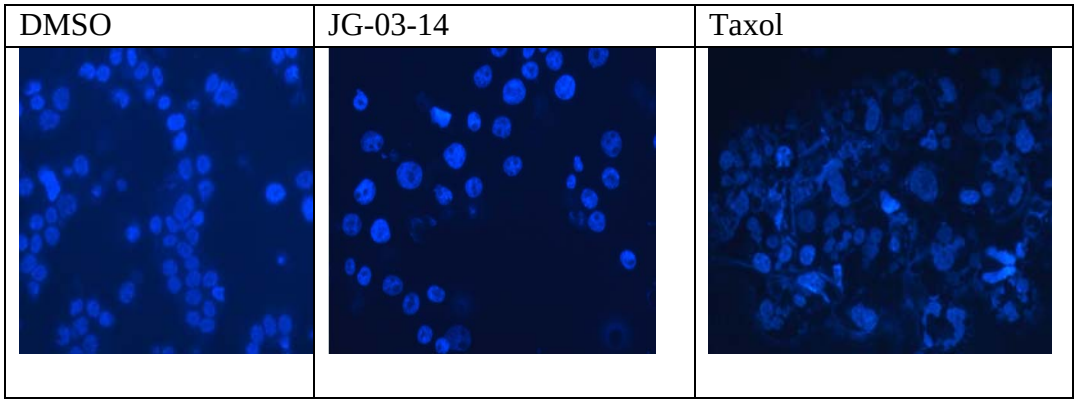

B.

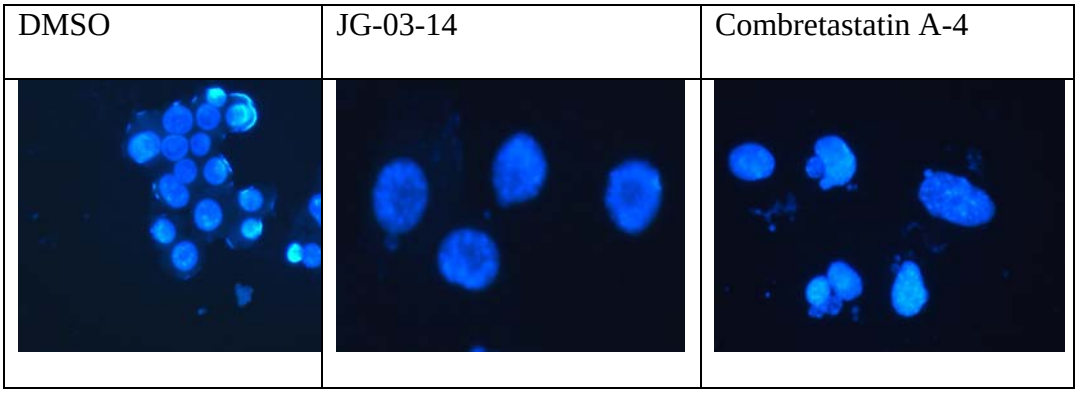

Figure 3. Images of HCT-116 cells exposed to JG-03-14. HCT-116 cells were treated with 500nM JG-03-14 for 72 hours. Apoptosis (nuclear fragmentation) and mitotic catastrophe (bi-nucleated cells with micronuclei) were evaluated based on morphology by DAPI (A) and Hoechst dye (B) staining, respectively. Magnifications shown are 200X and 400X, respectively.

A.

	Day 2	Day 3
DMSO	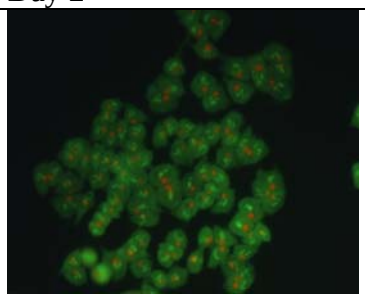	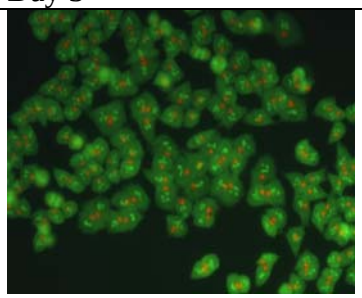
JG-03-14 (250 nM)	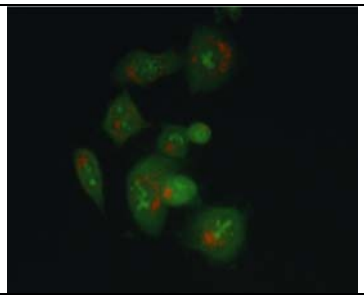	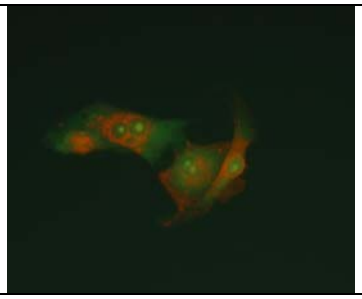

B.

MDC	DMSO	JG-03-14 (250 nM)	JG-03-14 (500 nM)
Day 3		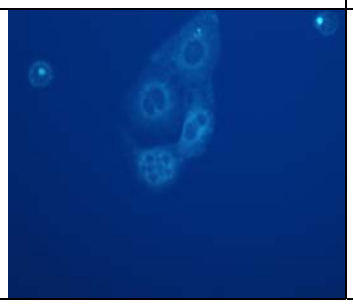	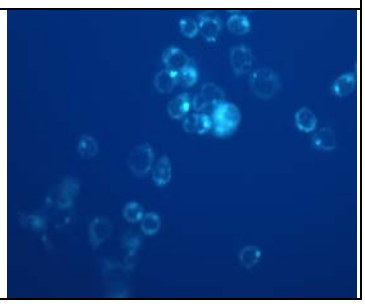

Figure 4. Staining for autophagy in HCT-116 cells exposed to JG-03-14. HCT-116 cells were treated with 500nM JG-03-14 continuously and autophagy was assessed based on acridine orange staining (A) and monodansylcadaverine staining (B) at 48 and 72 hr. Magnifications shown are 200X.

A.

	Day 2	Day 3
DMSO	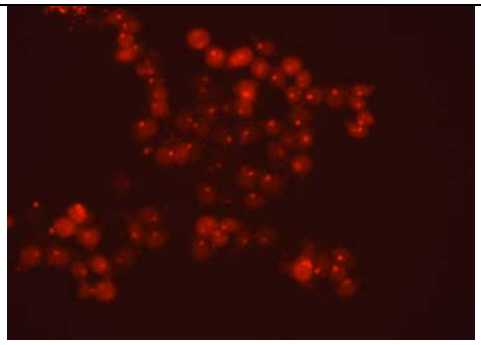	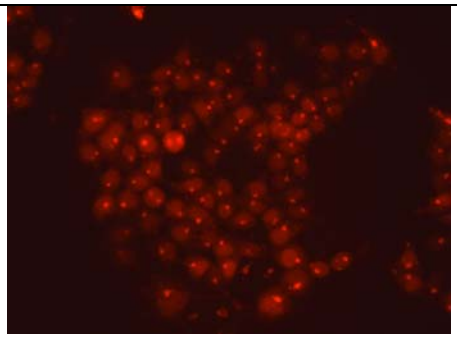
JG-03-14 (250 nM)	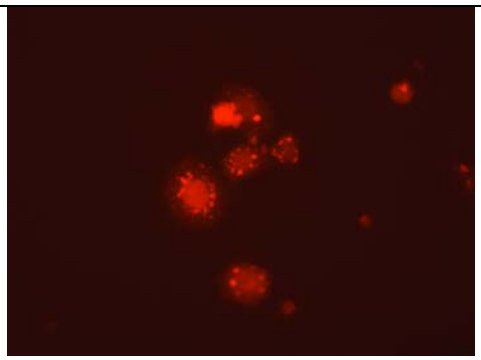	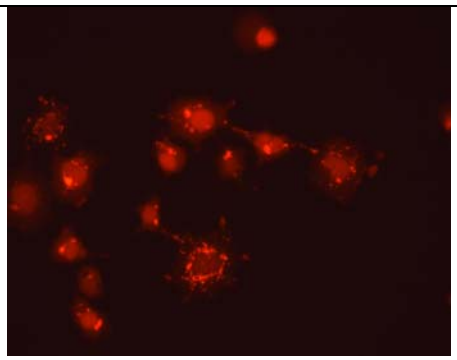
JG-03-14 (500 nM)	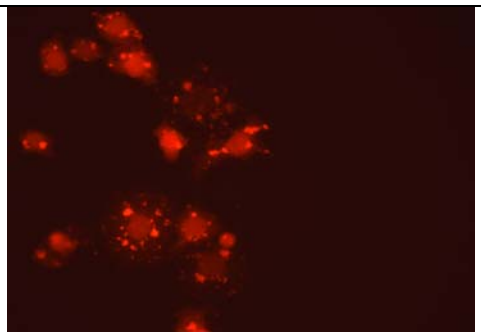	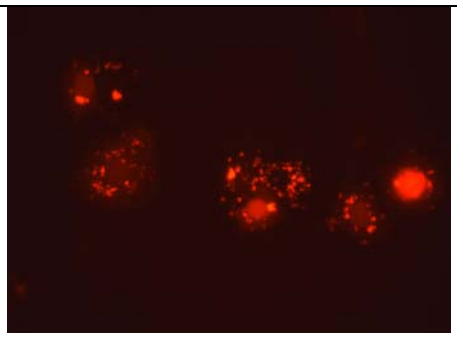

Figure 5. Confirmation of autophagy by JG-03-14 in HCT-116 cells. HCT-116 cells were treated with 500nM JG-03-14 continuously and autophagy was assessed based on redistribution of RFP-LC3 (A) and electron microscopy (B) at 48 and 72 hr. Magnifications shown as 200X for RFP, and a representative scale-bar for EM. Autophagic flux (C) was assessed based on the degradation of p62 and all treatments were performed for 48 hours. Chloroquine was used either independently or concurrently at 10 μM.

	DMSO	JG-03-14 (500 nM)
Day 3	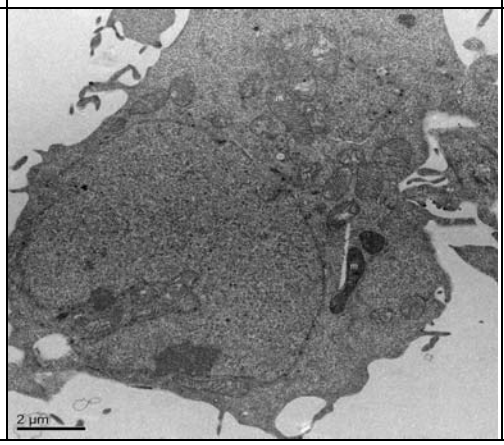	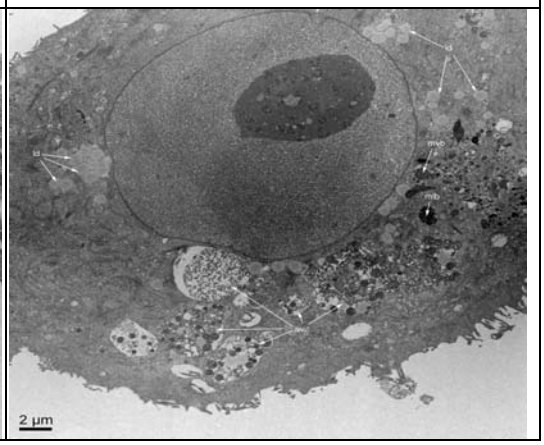

B.

C.

DMSO	CQ 10 uM	JG 500 nM	JG + CQ	Starved

P62

beta-actin

A.

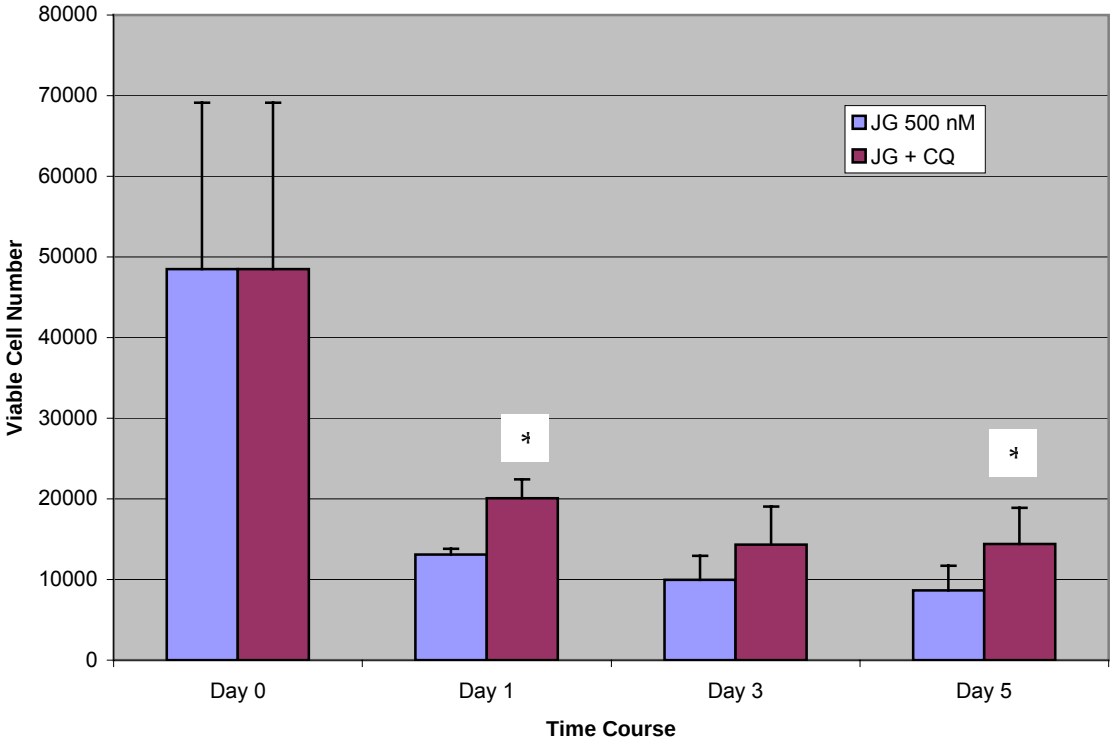

Figure 6. Influence of chloroquine on sensitivity to JG-03-14. HCT-116 cells were continuously exposed to 500 nM JG-03-14, 10 μM Chloroquine, or the combination treatment for the indicated times. Trypan blue was utilized for measure of cell viability (A), autophagy was visualized by MDC (B), and both adherent and non-adherent cells were collected for the TUNEL assay to measure apoptosis (C). Values shown are from a representative experiment with triplicate samples for each condition. Studies were reproduced in two additional replicate experiments. Significance differences from DMSO treatment are indicated by * ($P<0.05$) and were assessed by the two-way ANOVA and Fisher's PLSD post-hoc.

B.

DMSO	JG-03-14, 500nM	CQ 10 µM	JG-03-14 + CQ
		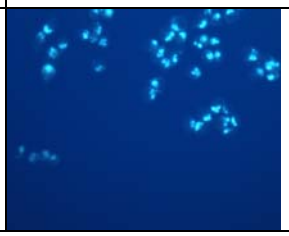	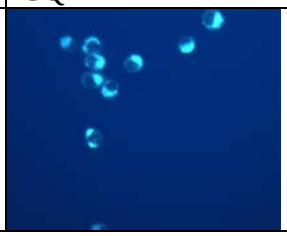

C.

	Day 3	Day 5
DMSO		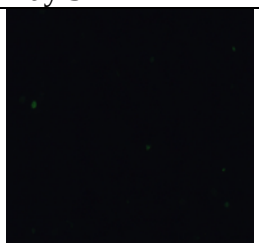
JG-03-14	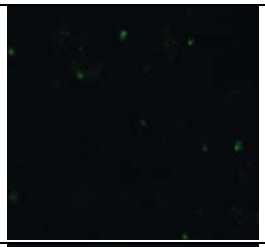	
CQ		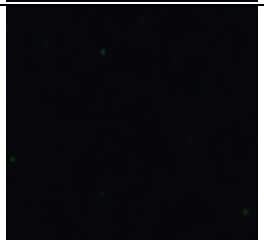
JG-03-14 + CQ	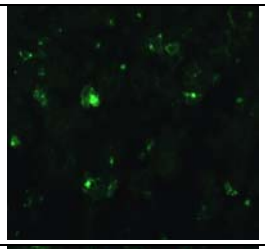	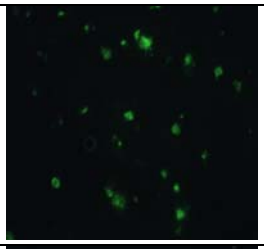
CA4	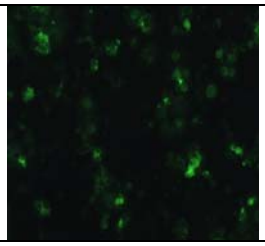	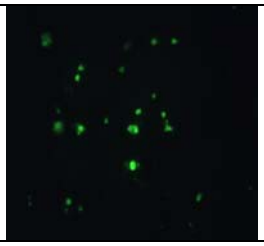

A.

	Day 3	Day 6	Day 9
DMSO	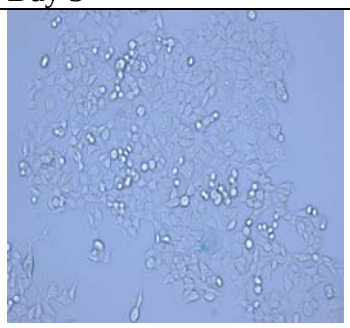	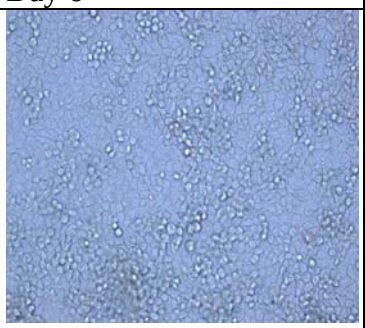	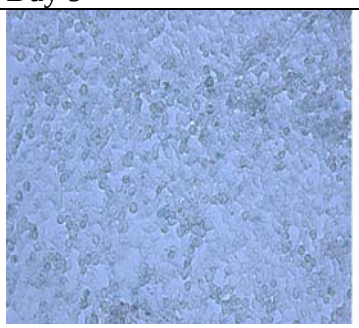
JG-03-14 (500 nM)	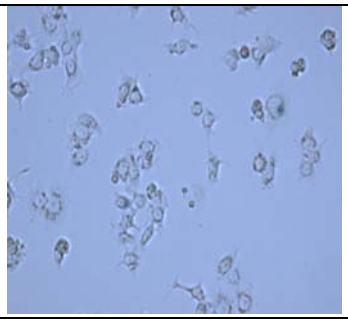	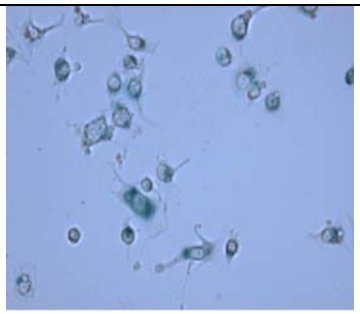	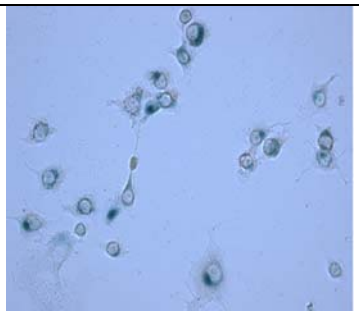

Figure 7. Induction of senescence and lack of proliferative recovery in HCT-116 cells treated with JG-03-14. HCT-116 cells were treated with 500nM JG-03-14 for 72 hours, drug was removed and replaced with drug free medium. Medium was replaced every 3 days. **A**. Senescence in residual surviving cells by beta-galactosidase staining. **B**. Three representative fields were quantified and counted as postive or negative for beta-galactosidase staining. **C.** Viable cell number. Significance differences from DMSO treatment day 3 are indicated by * ($P<0.05$) and were assessed by the two-way ANOVA and Fisher's PLSD post-hoc.

B.

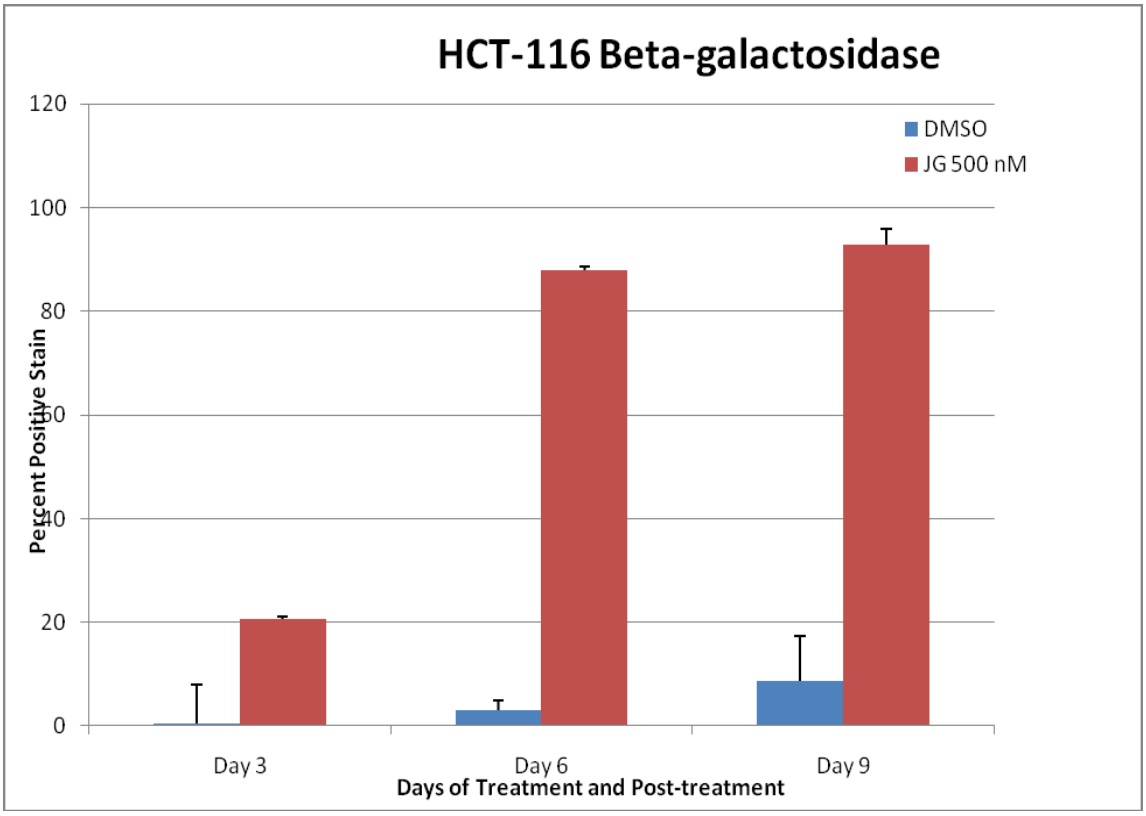
HCT-116 Beta-galactosidase
120
100
80
60
40
20
0
Percent Positive Stain
DMSO
JG 500 nM
Day 3
Day 6
Day 9
Days of Treatment and Post-treatment

C.

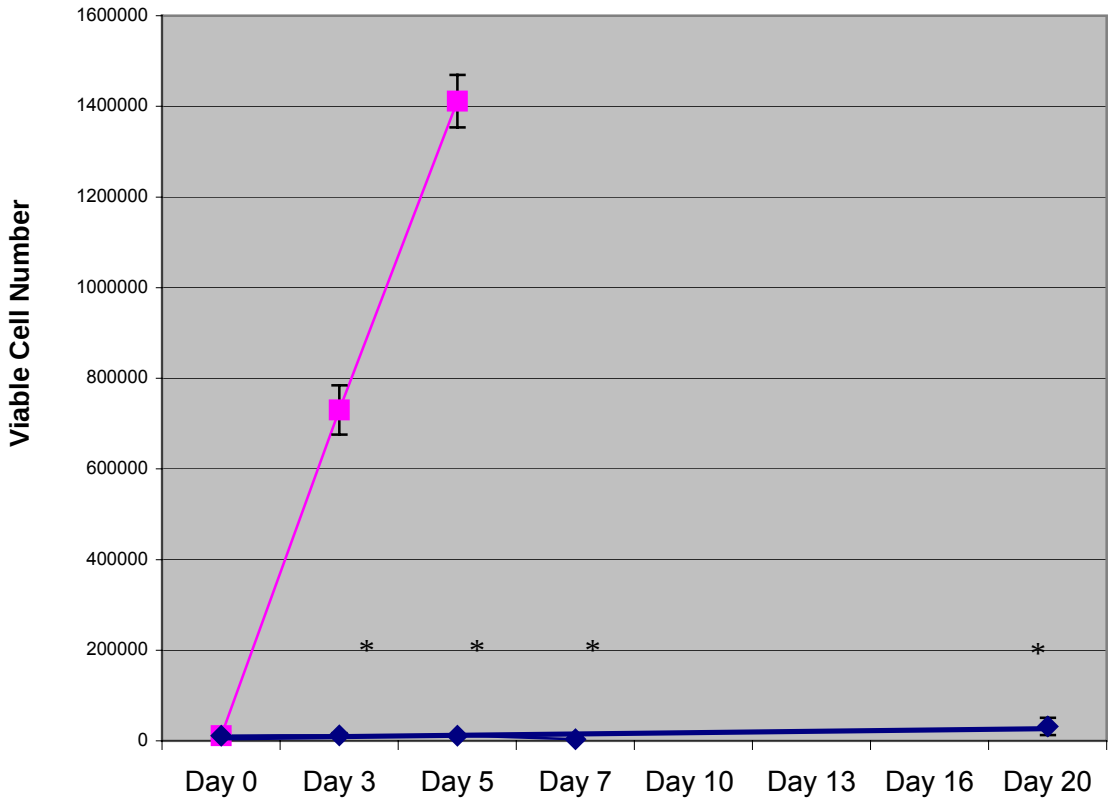
Viable Cell Number
1600000
1400000
1200000
1000000
800000
600000
400000
200000
0
Day 0
Day 3
Day 5
Day 7
Day 10
Day 13
Day 16
Day 20
*
*
*
*

ROS	DMSO	JG 500 nM	Taxol 100 nM	Combretastat in A-4 100 nM
Natural Light	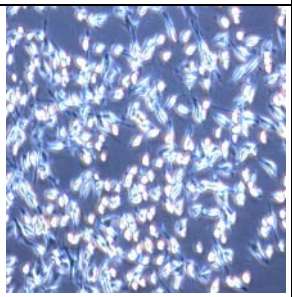	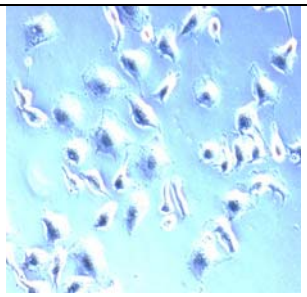	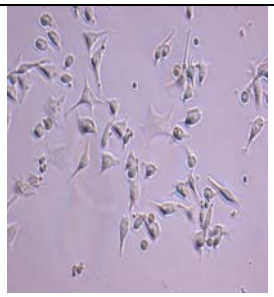	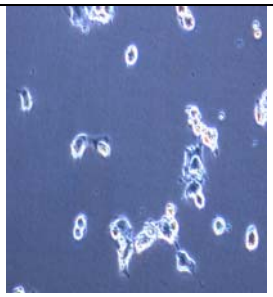
Stained	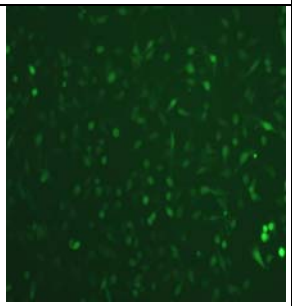	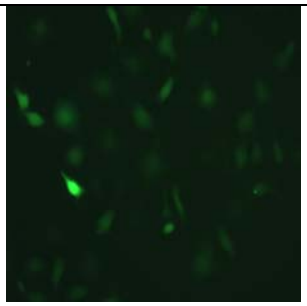	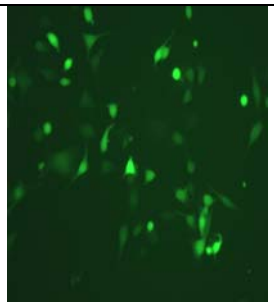	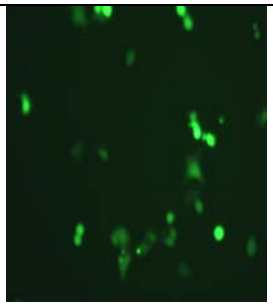

Figure 8. **DCF stain Assessment of Induction of Reactive Oxygen Species.** HCT-116 cells were continuously exposed to 500 nM JG-03-14, 100 nM taxol and 100 nM combretastatin A-4. Residual cells were stained using DCF fluorescent stain and images were taken at 400x magnification.

Results B. Effects of JG-03-14 in B16F10 melanoma cells

I. Effects of JG-03-14 on viability of B16F10 murine melanoma cells.

In an effort to extend the utility of the JG-03-14 compound to additional tumor models; studies of drug action were performed in B16F10 murine melanoma cells. Figure 9 indicates that JG-03-14 produced a concentration-dependent reduction in clonogenic survival, with substantial effects evident at concentrations of 250 and 500nM, similar to what was reported previously in breast tumor cells (Arthur, 2007).

Table II indicates that there was a reduction of 96% and 97% when B16F10 cells were exposed for 72 hours to 250 nM and 500 nM JG-03-14, respectively. All subsequent studies were performed using JG-03-14 at concentrations of either 250 nM or 500 nM (Table II).

II. Cell death induced by JG-03-14.

The previous clonogenic survival assay indicates a single cells ability to form a colony with exposure to JG-03-14. Therefore, we also monitored the effects of JG-03-14 on cell viability over a period of 5 days by simple trypan blue

exclusion. Figure 10 shows a time dependent decline in viable cell number when B16F10 cells were treated by continuous exposure to JG-03-14 at 500nM, a concentration that was previously found to be effective in promoting growth arrest and cell death in breast tumor cells (Arthur, 2007). The figure inset clearly demonstrate that the tumor cells exposed to JG-03-14 were dying as early as day 3, and that approximately 55% of the melanoma cells were lost after a period of 3 days.

III. Assessment of apoptosis

In previous studies, we have reported that JG-03-14 promotes primarily autophagy in p53 wild type MCF-7 cells and both autophagy and apoptosis in p53 mutant MDA-MB231 cells. As B16F10 melanoma cells are wild type in p53, it was our expectation that autophagic cell death would also be the primary mode of cell death. However, in order to examine the possibility that the cell death observed in B16F10 melanoma cells might be due to apoptosis, nuclear morphology was evaluated by DAPI staining. Figure 11A shows the untreated vehicle control with a clearly defined intact nucleus. With a few isolated exceptions, the nuclei of cells treated with JG-03-14 were intact although significantly enlarged in comparison to control cells. These cells also did not present evidence of mitotic catastrophe, where bifurcated cells have micronuclei resulting from aberrant mitosis (Figure 11B).

We also assessed the effects of other microtubule poisons (taxol, and combretastatin A-4, both at 100 nM) based on other publications and utilized

these poisons as positive controls for apoptosis. DAPI staining showed that the majority of nuclei were fragmented by taxol treatment after three days (Figure 11A). Combretastatin treatment appeared to promote mitotic catastrophe (Figure 11B). Consequently, the actions of JG-03-14 in terms of promoting cell death appear to differ markedly from that of these other microtubule poisons. Although some apoptotic bodies were detected in response to JG-03-14, the percentage was minimal and in no way could account for the amount of cell death seen following treatment.

In order to further understand the effects of JG-03-14 on B16F10, we used propidium iodide staining and single cell flow cytometry to quantify the cell cycle alterations induced by this novel microtubule poison.

IV. Cell cycle effects of JG-03-14

The next series of experiments was designed to verify the absence of apoptosis based on the detection of a cell population with DNA content lower than 2N, indicative of the DNA fragmentation that is a hallmark of apoptosis. FACS analysis confirmed that only a small fraction of the cell population could be detected in the sub G1 phase both at 24 and 72 hours following the initiation of treatment with 500 nM JG-03-14 (Figure 12). Again, using treatment with taxol and combretastatin as positive controls, we detected substantial populations of sub G1 cells after treatment with these microtubule poisons. These studies

confirm that apoptosis likely played only a minor role in cell death induced by JG-03-14 in the B16F10 melanoma cell line.

Figure 4 also presents an analysis of cell cycle distribution of B16F10 cells treated with JG-03-14. JG-03-14 transiently arrested the p53 wild type tumor cells in the G2/M cell phase after the first day of treatment, and this G2/M block persisted for at least 72 hours. After 72 hours, the cell cycle distribution shifted, with 38.9% of the cells in G2/M and 14.7% in G1/S. Of particular interest was the observation that these p53 wild type cells appear to continue to replicate their DNA following the G2/M arrest, resulting in a hyperdiploid population. This effect was observed after the first day of treatment and the hyper diploid cell population had more than doubled after 72 hours, where 29.7% of the B16F10 cells were polyploid.

As indicated above, FACS analysis determined that after 24 hours a very large population is in G2/M arrest. However, after 72 hours there is a small population of cells that are sub-G1. This percent population does not correlate with the extent of cell death observed. This apparent apoptosis independent cell death indicated that it was important to assess alternative pathways for cell killing such as mitotic catastrophe and autophagy.

V. Assessment of mitotic catastrophe in B16F10 melanoma cells after JG-03-14 treatment

Since apoptosis could only account for a small fraction of the cell death observed in the B16F10 melanoma cells upon treatment with JG-03-14, it appeared likely that other modes of cell death such as mitotic catastrophe or autophagy might be responsible for the time dependent decline in cell number observed in the studies presented in Figure 10. Due to the presence of enlarged cells and a hyper-diploid cell population we considered the possibility of mitotic catastrophe being the mode of cell death in B16F10 cells. However as shown in figure 11B, analysis using Hoechst stained cells failed to detect evidence of bi-nucleated cells and micronuclei that are characteristics of mitotic death (DeMasters et al, 2006)

VI. Induction of autophagy by JG-03-14.

In our previous work, the p53 wild type MCF-7 and p53 mutant MDA-MB-231 breast tumor cells demonstrated essentially similar sensitivity to JG-03-14; however, their response was different with regard to the modes of cell death. As in the current studies, MCF-7 cells were not dying through apoptosis based on FACS analysis and the TUNEL assay, but rather through autophagy while the p53 mutant MDA-MB231 cells demonstrated both apoptosis and autophagy. Consequently, we assessed the promotion of autophagy by JG-03-14 using a number of assays including acridine orange and monodansylcadaverine staining, and electron microscopy.

Figure 13A shows a quite extensive level of basal autophagy in the B16F10 melanoma cells based on the mosaic distribution in control cells, which is consistent with a recent time-lapse GFP-LC3 by Tormo et al., (2009). However, treatment with JG-03-14 resulted in an increase in puncta formation throughout the cell, consistent with the formation of acidic vesicles.

To confirm the promotion of autophagy, we used an additional approach, staining of autophagic vesicles with monodansylcadaverine, a stain that binds to the lipid membrane of the autophagosomes (Niemann et al., 2001). Figure 13B shows a similar pattern to what was observed with the acridine orange staining. Specifically, the controls show a more condensed pattern of vacuoles while the cells treated with JG-03-14 show a highly distributed punctuate pattern throughout the cytoplasm. The cells treated with other microtubule poisons did not show enhanced formation of autophagic vesicles (Figure 13A and 13B).

Another mechanism for detection of autophagic vesicles is the use of electron microscopy (Figure 14). Here we show that the control cells there are clearly intact mitochondria and a healthy nucleus. The B16F10 cells that have been treated with JG-03-14 (500 nM) show clear nuclear and cell enlargement as well as induction of autophagic vesicles that commence degradation of damaged cellular constituents.

VIII. Effects of autophagic inhibitors on the response to JG-03-14 treatment in B16F10 cells

There is continuing controversy in the literature as to whether autophagy is a cytoprotective mechanism or an actual mode of cell death (Mori et al, 2007; Boya et al, 2005). In a further attempt to confirm the mode of cell death caused by JG-03-14 and to elucidate the ambiguous role of autophagy, we sought to block autophagy. In efforts to address this question, cells were pre-treated or concurrently treated with 3-methyladenine (3-MA), Wortmannin, LY-249004, Bafilomycin A-1 and Chloroquine, all of which have been shown to inhibit autophagy in a variety of experimental systems (Meschini et al, 2008; Seglen and Gordon, 1982; Shacka et al., 2006). However, many of these agents had intrinsic toxicities making it difficult if not impossible to study the effects of autophagic inhibition (data not shown). The late inhibition of H-ATPase pump with Bafilomycin did seem to partially prevent the acidification of autophagic vesicles in concurrent treatment with JG-03-14 (Figure 15A). Consequently, studies were conducted using Bafilomycin A-1 at 10 nM. Figure 15B shows that Bafilomycin produced a modest protection against the cytotoxic effects of JG-03-14 in both the MTT absorbance assay as well as the Trypan Blue assay for cell viability. The fact that protection was relatively modest can be explained by the observed increase in the amount of apoptotic cells by DAPI staining (Figure 15C).

VIII. Promotion of senescence and lack of proliferative recovery in residual cells

In previous studies, we have reported that residual cells that appear to have survived the drug treatment were in a state of senescence arrest (Arthur et al. 2007); in some studies, senescence has been succeeded by proliferative recovery (Elmore et al. 2005). In the current studies, we observe that 95% of the residual cell populations following treatment with 500 nM JG-03-14 are arrested in senescence, based on beta-galactosidase staining as well as cell enlargement and spreading (Figure 16A). Similarly, 91% of the cells treated with 250 nM JG-03-14 appeared to be senescent. The induction of senescence could be observed as early as day 2. Adriamycin was used as a positive control for senescence.

In order to determine whether the cells had lost self-renewal capacity, drug was removed after 72 hours and cell number was followed for an additional 17 days. We failed to detect any evidence of cell re-growth for periods as long as the study, 20 days total, indicating that the cells had lost all reproductive capacity (figure 16B).

IX. Relationship between Autophagy and Senescence

A recent review by Young et al. gave insight into the relationship between autophagy and senescence. Therefore we wanted to investigate whether or not the inhibition of autophagy in this model would have an effect on senescent cells. Our studies also revealed that through the inhibition of autophagy, we were able to attenuate senescence based on beta-galactosidase staining (Figure 15D).

Analysis of the images showed a 60% reduction in positive staining cells (Figure 15E). Interestingly, this attenuation of senescence did not appear to protect cells from loss of proliferative capacity (Figure 16B), but does shine light on the possibility of shared pathways between autophagy and senescence. This population of senescent cells was quantified and presented reduction of 95% to 38.7% and 91% to 27% for combination JG-03-14 at 500 nM and 250 nM with Bafilomycin, respectively (Figure 15E). This indicates that the combination treatment is also promoting an alternative mode of cell death, that of apoptosis.

X. Evaluation of JG-03-14 effect on cardiac cell viability

To assess the potential toxicity accompanying the cancer cell killing effects of JG-03-14, we employed an immortalized in vitro cardiac model, H9c2 cardiomyocytes (Zordoki & El-Kadi, 2007). Combretastatin is a microtubule poison currently under clinical investigation and has been shown to promote extensive cardiotoxiticy (Stevenson et al., 2003). Therefore, we wanted to determine if our compound would have an advantage over the pronounced toxicities of combretastatin to the heart. Using the MTT dye assay, we found JG-03-14 is consistently less toxic than the other microtubule poisons investigated, combretastatin A-4 and taxol (Figure 17).

Table 2.

Table 1 – Clonogenic Survival assay following 72h JG-03-14 exposure (% control)		
	JG-03-14 (250nM)	JG-03-14 (500 nM)
B16F10	4.31 +/- 1.1*	2.7 +/- 0.65*
Values represent average colonies formed 2 weeks post 72 hours treatment JG-03-14 * P= >0.0001 compared to Control group		

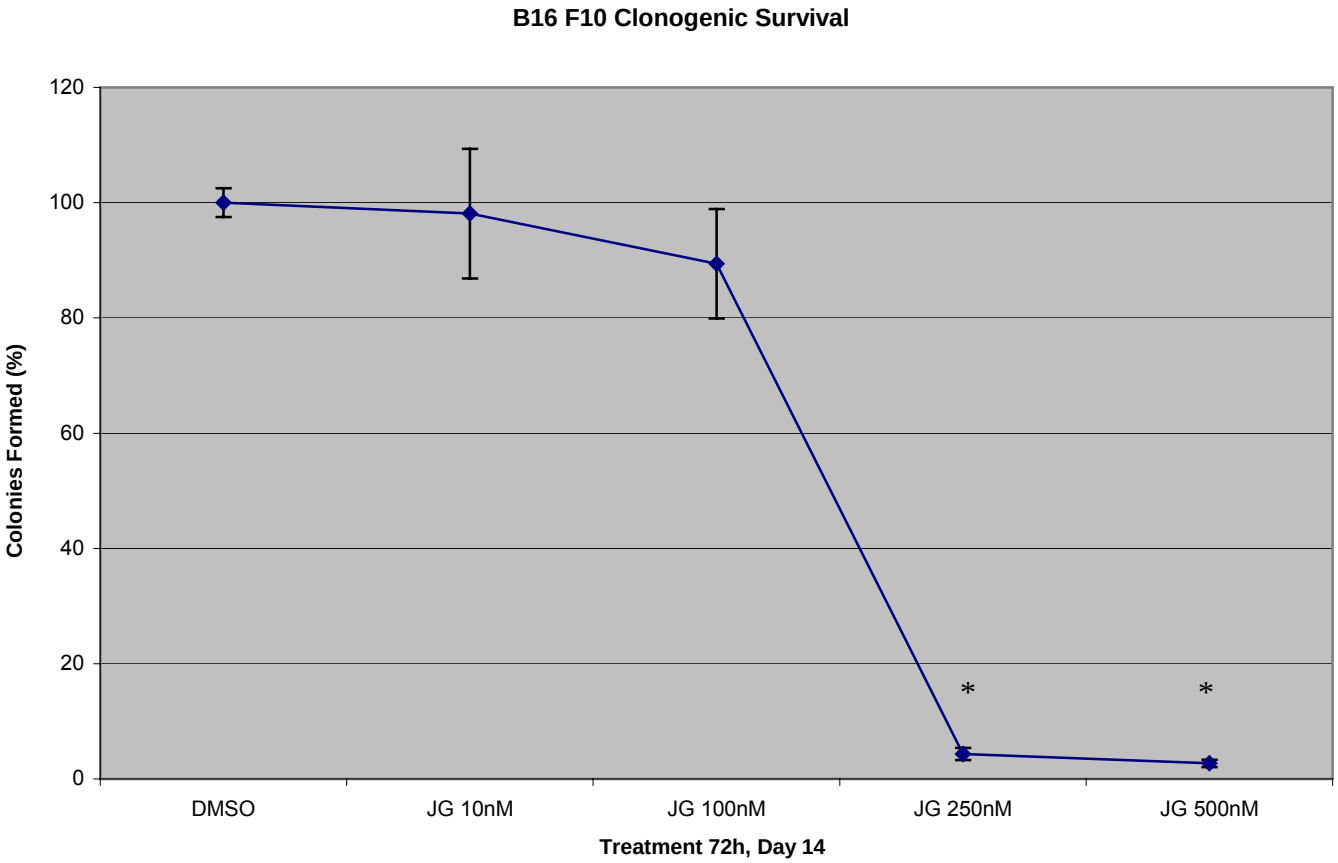

Figure 9. Dose-dependent Effects of JG-03-14 on B16F10 Clonogenic Capacity
B16F10 cells were plated based on previous dose responses. 100 cells for DMSO, JG 10 nM and 500 cells for JG 250 nM and JG 500 nM. Colonies were considered as greater than 10 cells and lacking the hallmarks of senescence. Assay shown is a representative experiment done in triplicate and was corrected for plating efficiency. Two identical replicate experiments were performed for confirmation. Error bars reflect standard deviations and significant differences from DMSO treatment are indicated by * ($P<0.05$), which were assessed by the ANOVA and Tukey/Kramer post-hoc analysis.

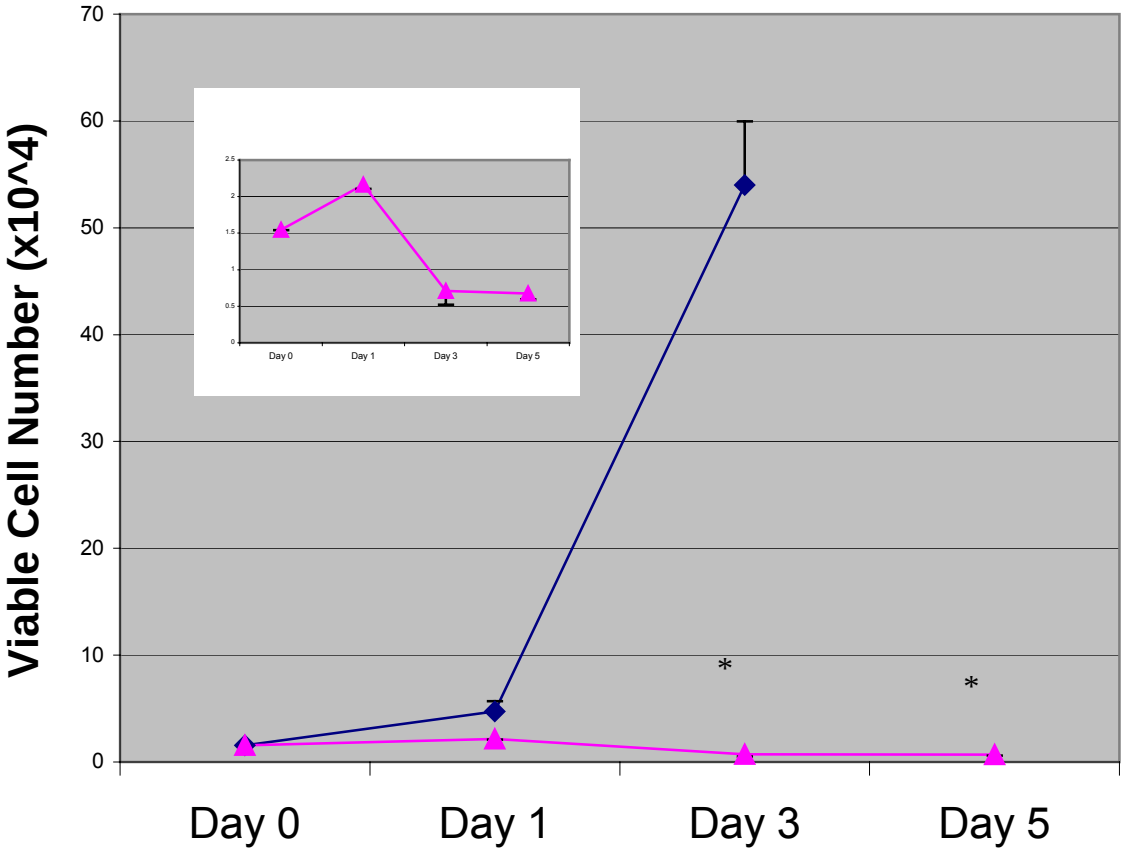

Figure 10: **Time dependent loss in cell viability by exposure to JG-03-14.** B16F10 cells were continuously exposed to 500nM JG-03-14 and viable cell number was monitored by trypan blue exclusion over a period of 120 hours. Values shown are from a representative experiment with triplicate samples for each condition. Studies were reproduced in two additional replicate experiments. The inset shows the decline in viable cell number using an expanded Y-axis. Significance differences from DMSO treatment are indicated by * ($P<0.05$) and were assessed by the Student t-test.

A.

	DMSO	JG-03-14 (500 nM)	Taxol (100 nM)
Day 3 200X	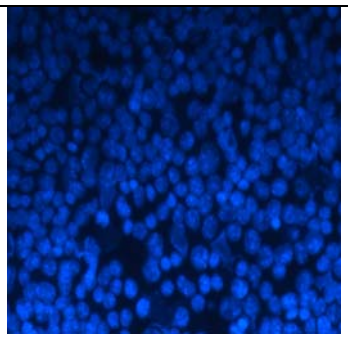	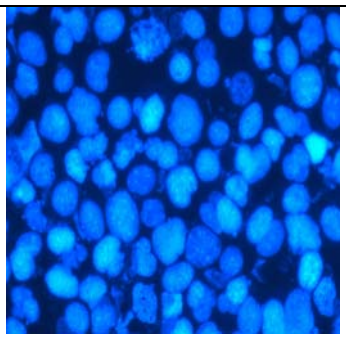	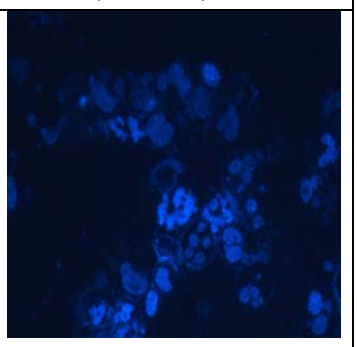

B.

	DMSO	JG-03-14 (500 nM)	Combretastatin A-4 (100 nM)
Day 3 200X	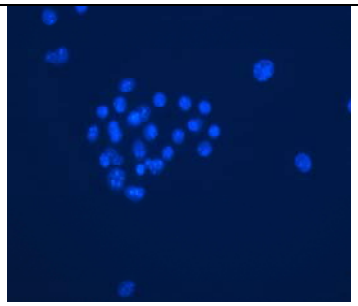	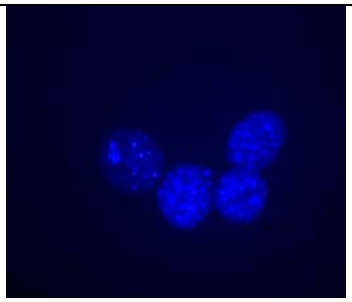	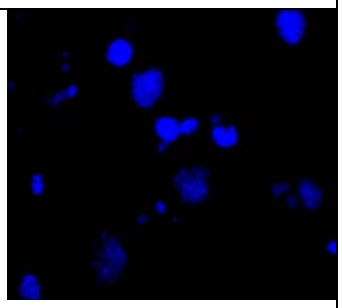
400X	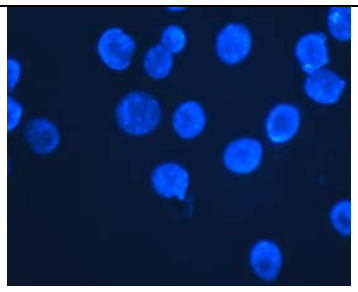	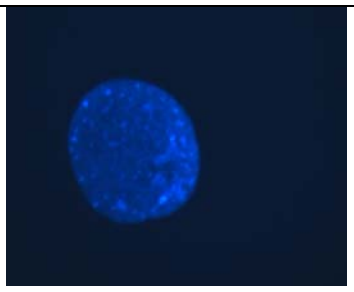	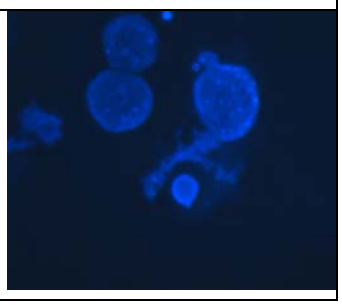

Figure11: **Images of B16F10 nuclear integrity of cells exposed to JG-03-14.** B16F10 cells were treated with 500nM JG-03-14 for 72 hours. Apoptosis and mitotic catastrophe were evaluated based on morphology by DAPI staining (A) and Hoechst (B) (nuclear fragmentation and bi-nucleated cells with micronuclei, respectively).

B16F10	Day 1	Day 3	Percent Population Day 1	Day 3
DMSO	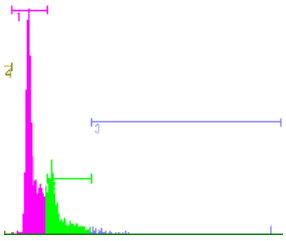	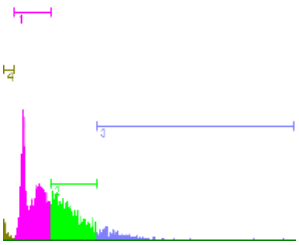	G1/S = 63.3% G2/M = 31% Sub G1 = 0.9% Hyperploid = 4.7%	G1/S = 49.1% G2/M = 37.3% Sub G1 = 2.7% Hyperploid = 11%
JG-03-14 (500 nM)	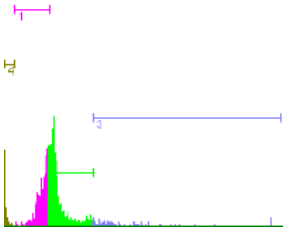	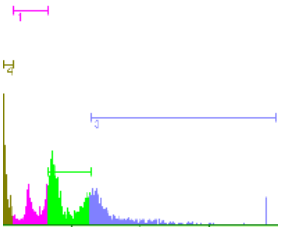	G1/S = 32.7%, G2/M = 49.5% Sub G1 = 6.7% Hyperploid = 11%	G1/S = 16.7% G2/M =38.9% Sub G1 = 14.7% Hyperploid = 29.7%
Combretastatin A-4 (100 nM)	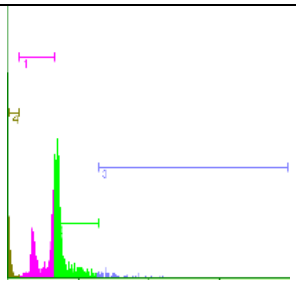	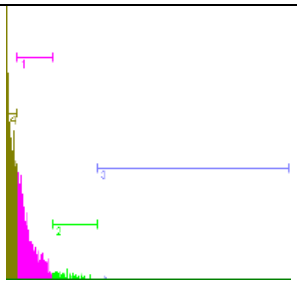	G1/S = 29% G2/M = 55.3% Sub G1 = 7.5% Hyperploid = 8.1%	G1/S = 43.8% G2/M = 5.4% Sub G1 = 49.3% Hyperploid = 1.6%
Taxol (100 nM)	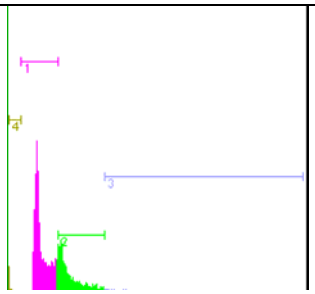	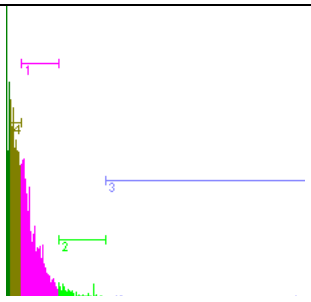	G1/S = 56.3% G2/M = 33.4% Sub G1 = 4.5% Hyperploid = 5.8%	G1/S = 50.5% G2/M = 5.7% Sub G1 = 42.7% Hyperploid = 0.9%

Figure 12: **Cell Cycle Distribution of B16F10 cells exposed to JG-03-14.** B16F10 cells were treated continuously with various microtubule poisons. Both supernantant and adherant cells were collected and analyzed using propidium iodide single cell analysis after both 24 hours and 72 hours.

A.

B16F10	Day 2	Day 3
DMSO	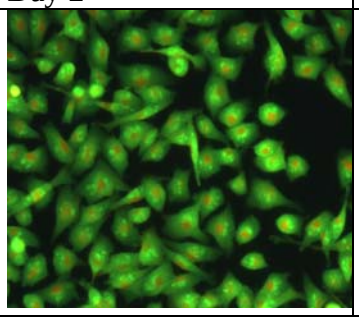	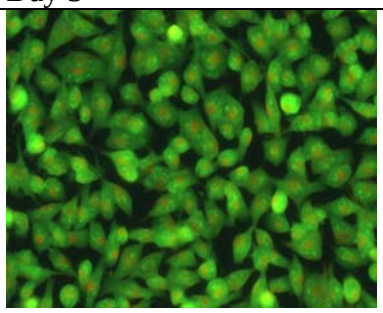
JG-03-14 (500 nM)	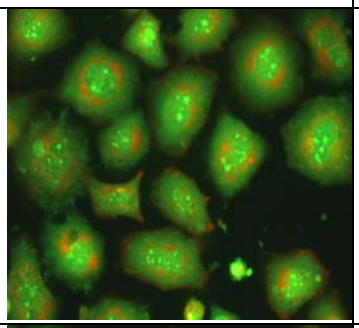	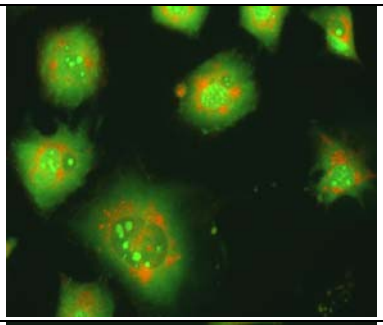
Taxol (50 nM)	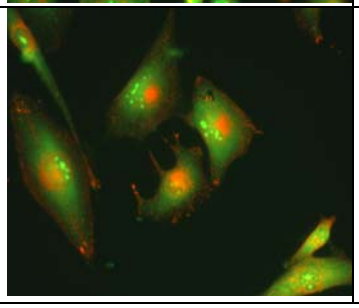	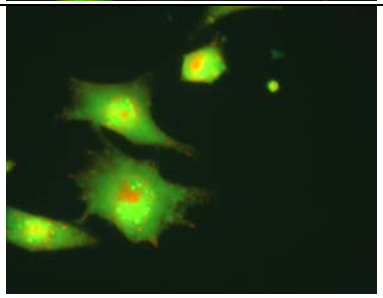

Figure 13. Assessment of autophagy in B16F10 cells exposed to JG-03-14 B16F10 cells were treated with Vehicle, 500nM JG-03-14, and 100 nM Combretastatin A-4 continuously and autophagy was assessed based on acridine orange staining 400X (A) and monodansylcadaverine 200X (B) staining at 72 hours.

B.

Day 3 MDC	DMSO	JG-03-14 (500 nM)	Combretastatin A-4 (100 nM)
		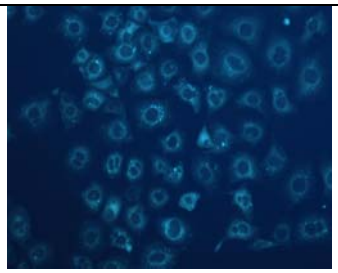	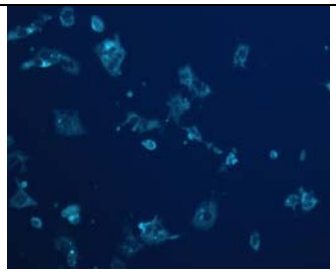

Electron Microscopy	B16F10
Control	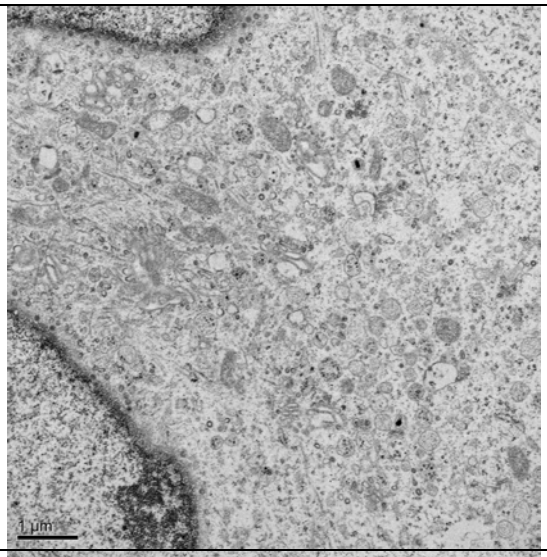
JG-03-14 (500 nM)	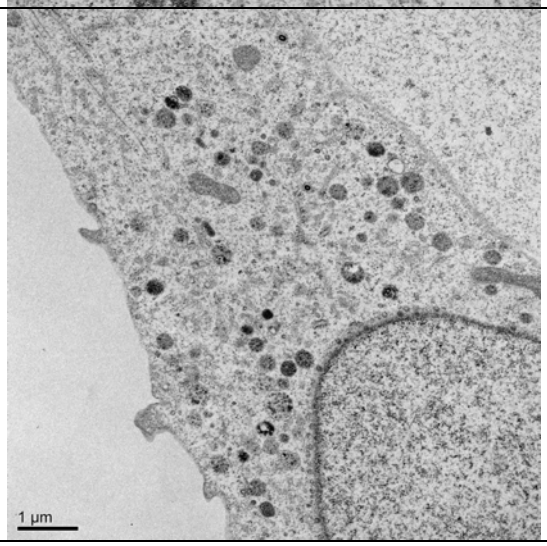

Figure 14: Confirmation of autophagy in B16F10 cells exposed to JG-03-14
Autophagy was confirmed using electron microscopy visualization. B16F10 cells were treated for 72 hours continuously prior to fixation and staining. Scale-bars indicate magnification comparisons for cell enlargement.

A.

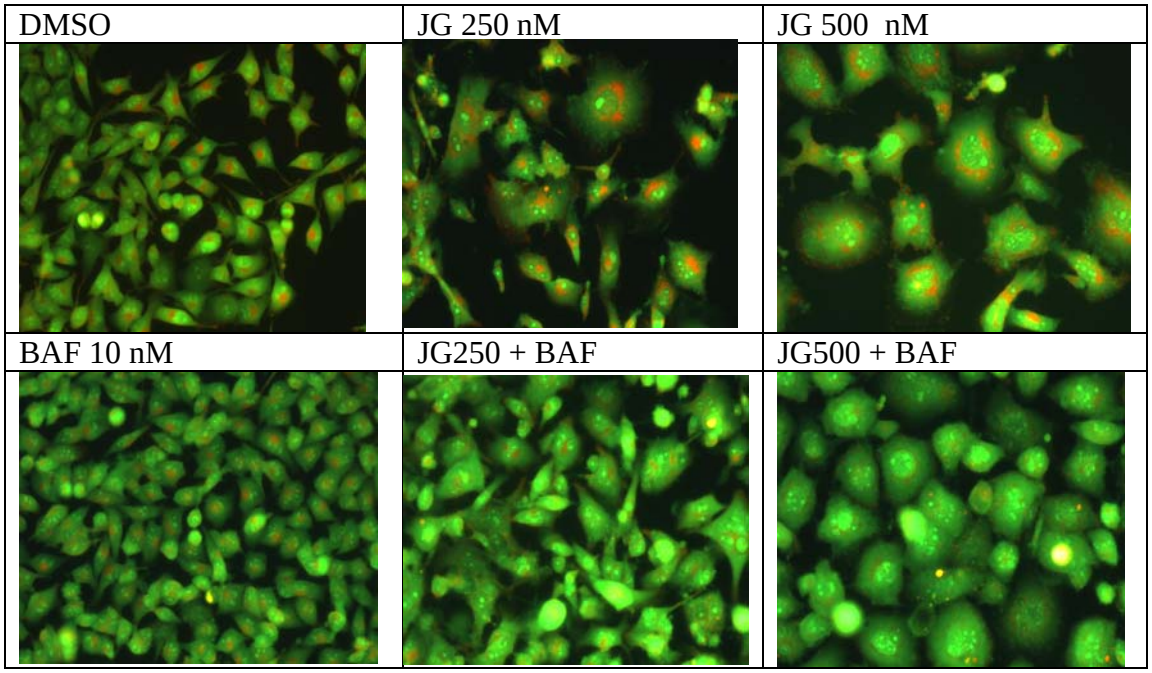

Figure 15. The effect of Bafilomycin on B16F10 response to JG-03-14 The B16F10 cells were exposed to either JG-03-14 250 nM or 500 nM and Bafilomycin 10 nM or in combination. Adriamycin and Taxol used as positive controls. Acridine orange staining was used as a measure of autophagy (200X) (A), as well as its protective effects on cell viability using trypan blue and MTT absorbance assays (B). Also shown is the effect the combination had on nuclear integrity as seen by DAPI (400X) (C), attenuating effects on senescence (200X) (D) and quantified blue positive staining (E). Viability assays are two replicate experiments combined each done in triplicate.

B.

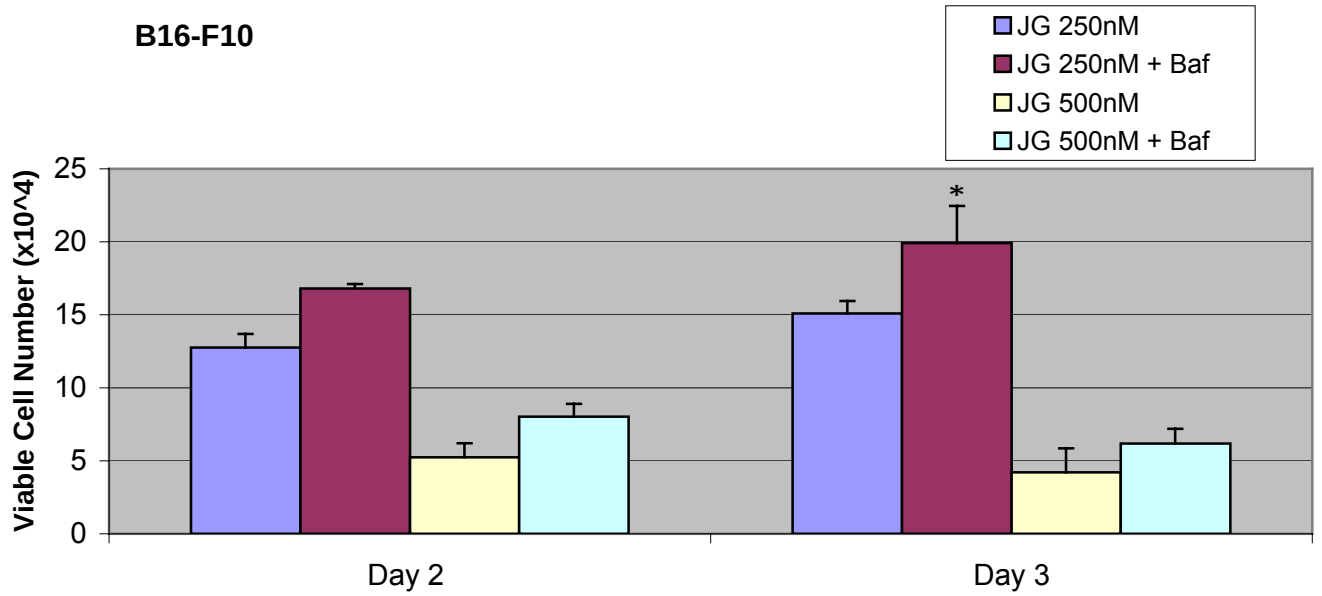
B16-F10
JG 250nM
JG 250nM + Baf
JG 500nM
JG 500nM + Baf
Viable Cell Number (x10^4)
25
20
15
10
5
0
*
Day 2
Day 3

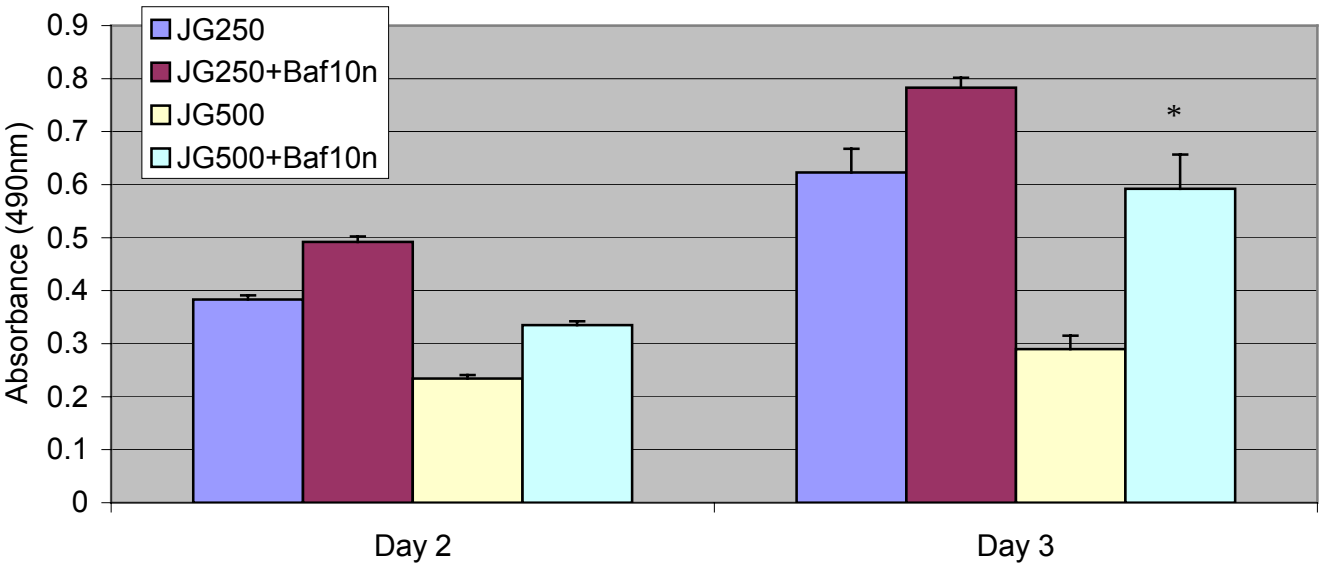
JG250
JG250+Baf10n
JG500
JG500+Baf10n
Absorbance (490nm)
0.9
0.8
0.7
0.6
0.5
0.4
0.3
0.2
0.1
0
*
Day 2
Day 3

C.

DMSO	JG 250 nM	JG 500 nM
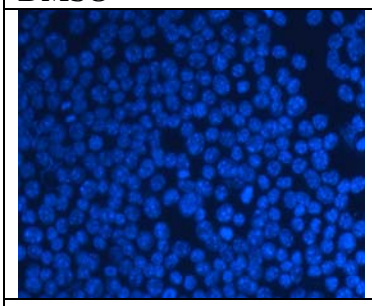	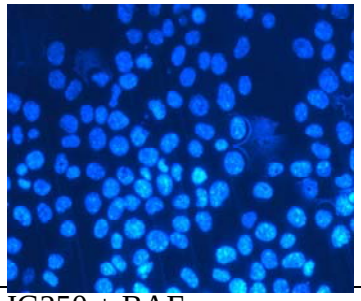	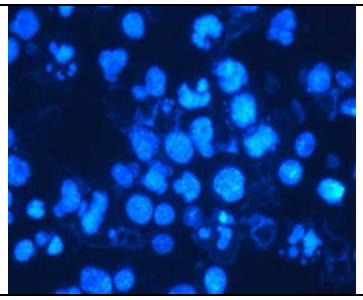
BAF 10 nM	JG250 + BAF	JG500 + BAF
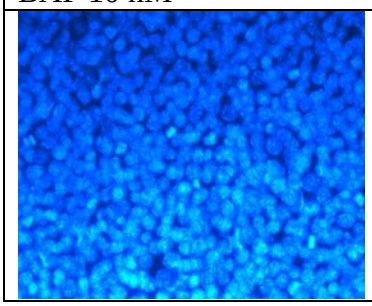	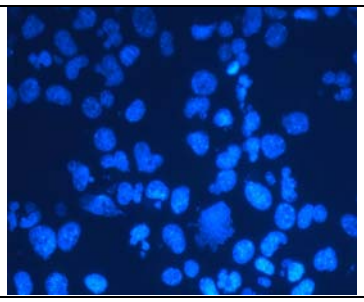	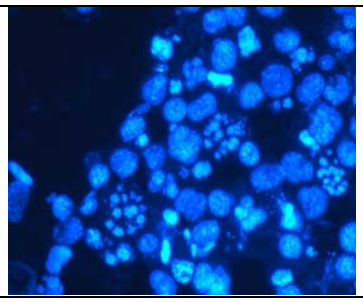

D.

DMSO	JG 250 nM	JG 500 nM
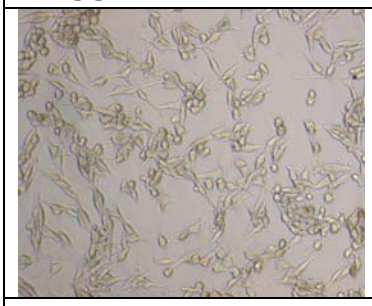	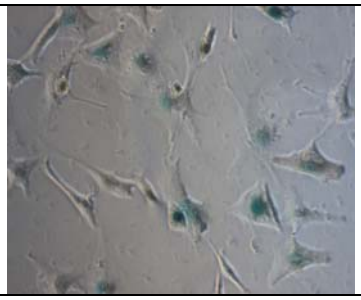	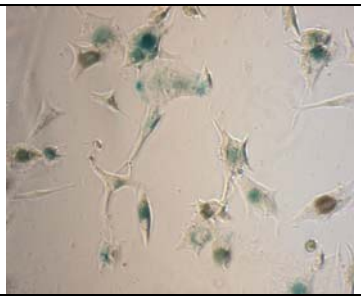
BAF 10 nM	**JG250 + BAF**	**JG500 + BAF**
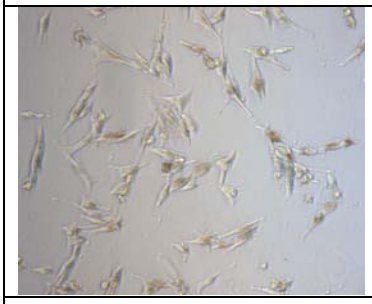		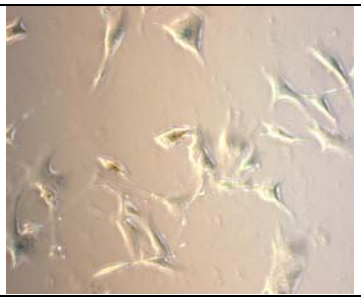
ADR 1μM		
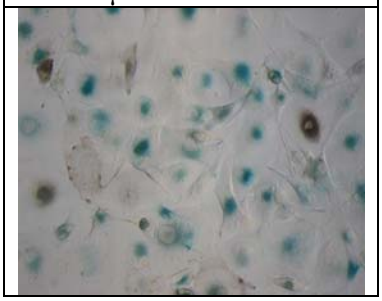		

E.

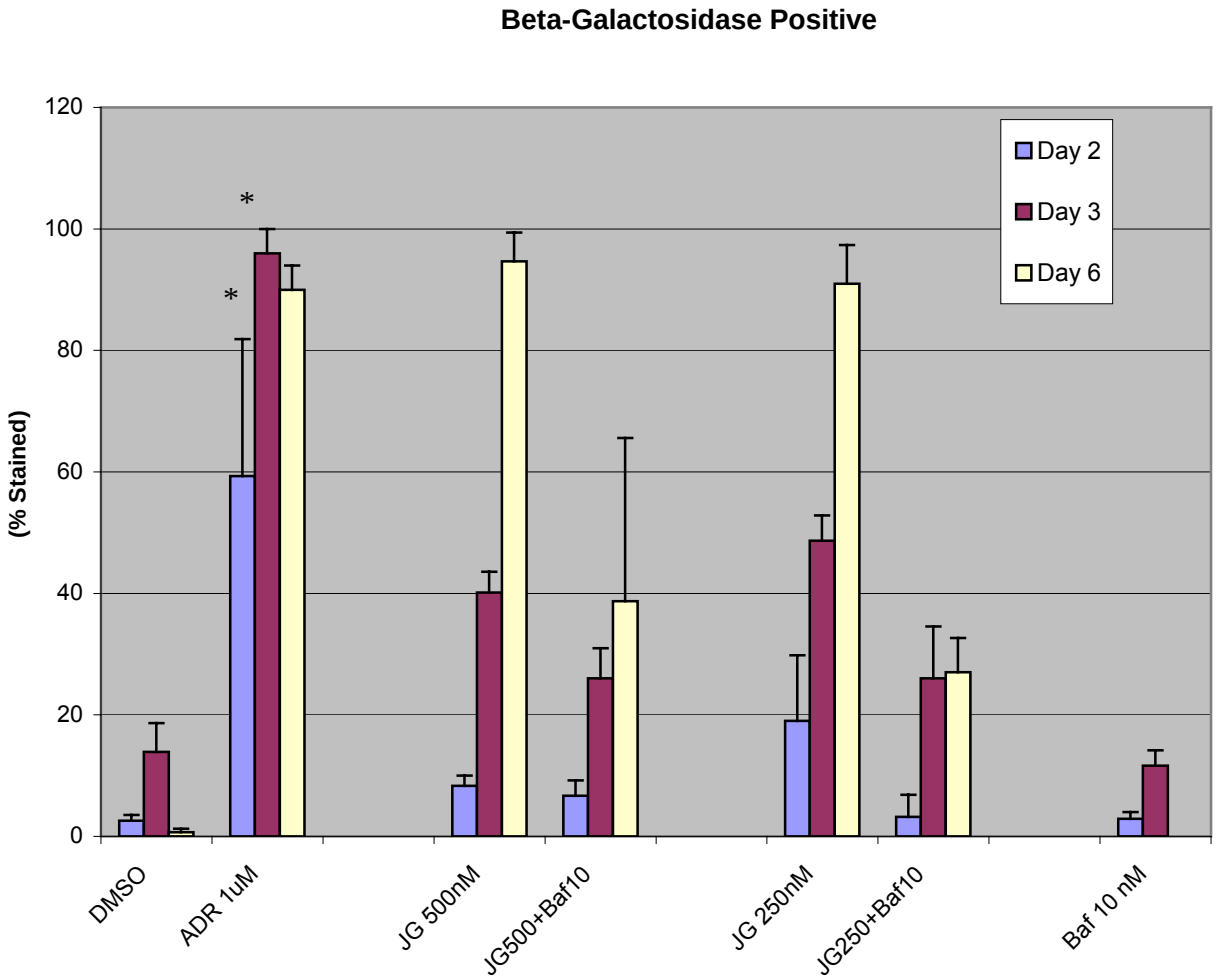
Beta-Galactosidase Positive
(% Stained)
120
100
80
60
40
20
0
Day 2
Day 3
Day 6
*
*
DMSO
ADR 1uM
JG 500nM
JG500+Baf10
JG 250nM
JG250+Baf10
Baf 10 nM

A.

B16F10 (10x	Day 2	Day 3	Day 6
Control - DMSO	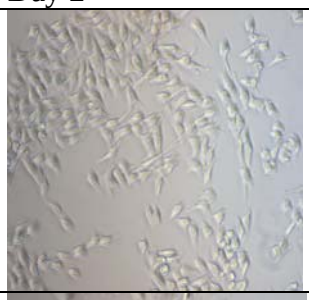		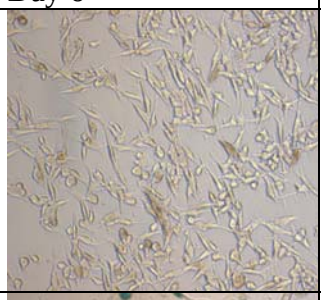
JG-03-14 (500 nM)			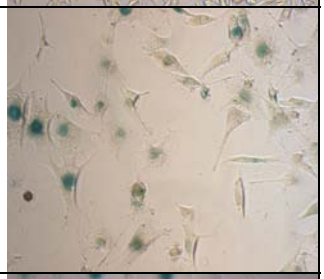
Adriamycin (1 uM)	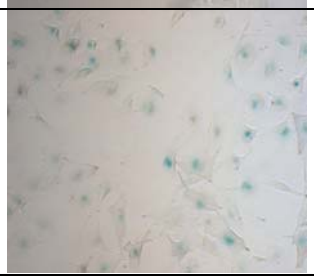		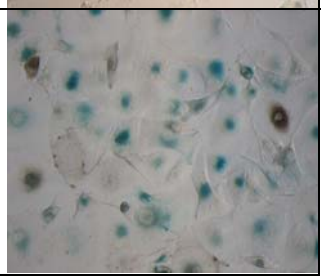

Figure 16: Senescence and destruction of proliferative recovery for B16F10 cells exposed to JG-03-14 B16F10 cells were treated with 500nM JG-03-14 for 72 hours, drug was removed and replaced with drug free medium. Medium was replaced every 3 days. Beta-galactosidase staining (A) and lack of proliferative recovery (B) is displayed as assessed using trypan blue trypan blue. Blue Diamonds (JG-03-14 500 nM), Maroon Triangles (JG + Bafilomycin 10 nM). Significant differences from DMSO treatment day 3 for both JG alone and Combination are indicated by * ($P<0.05$) and were assessed by the two-way ANOVA and Fisher's PLSD post-hoc.

B.

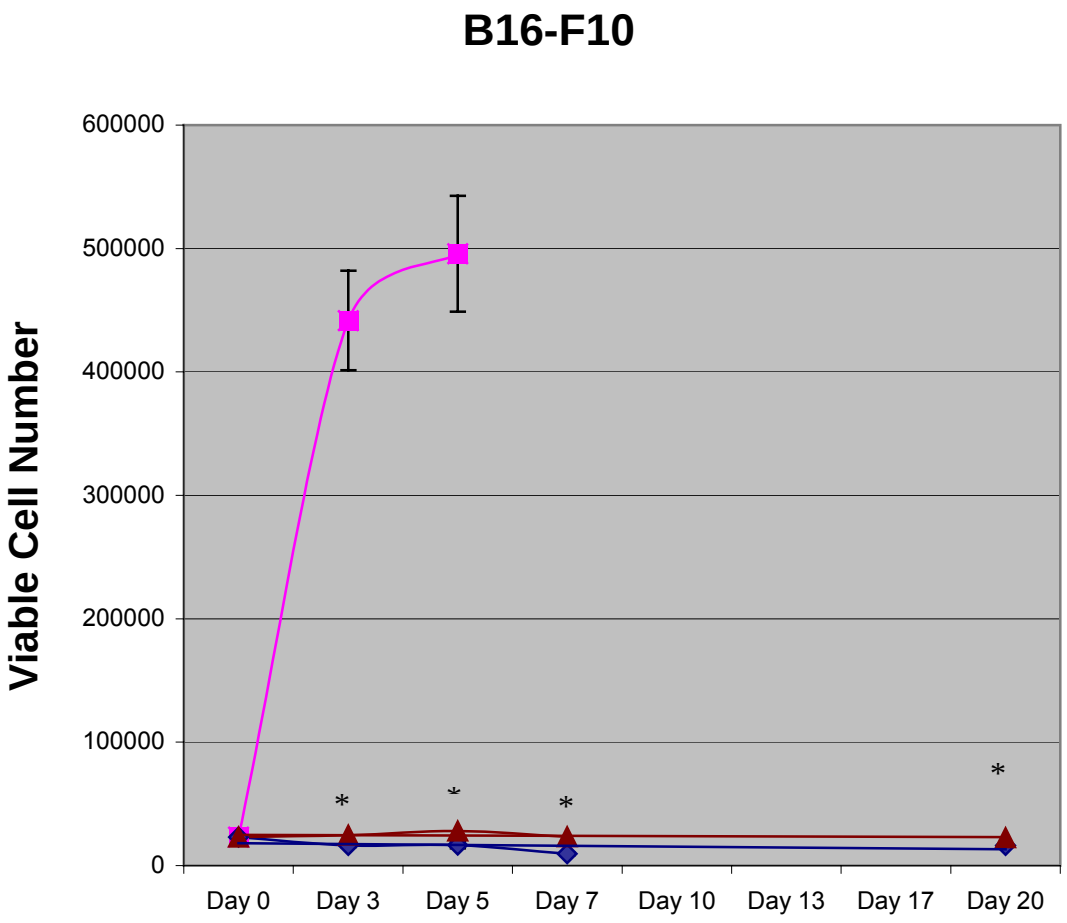
B16-F10
Viable Cell Number
600000
500000
400000
300000
200000
100000
0
Day 0
Day 3
Day 5
Day 7
Day 10
Day 13
Day 17
Day 20
*
*
*
*

.

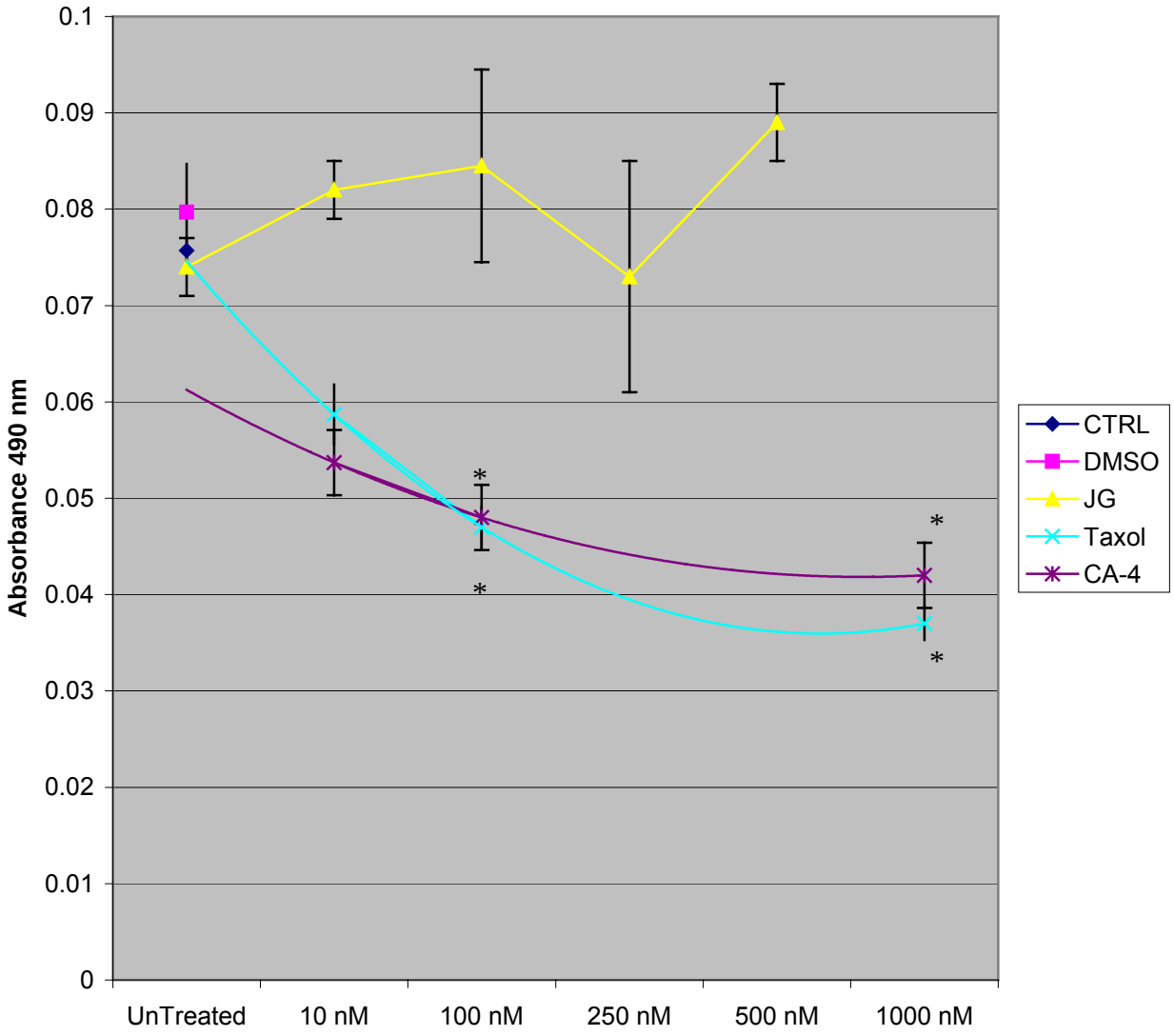

Figure 17: Effects of microtubule poisons Taxol, Combretastatin A-4 and JG-03-14 on H9c2 rat embryonic cardiomyocytes. H9c2 cells were treated dose dependently with nano molar concentrations of JG-03-14, Taxol and Combretastatin A-4. MTT absorbance assay shows a concentration dependent decline in viable cell number. Shown is a representative experiment performed with samples in triplicate. An identical replicate experiment was performed to confirm results. Significant differences from DMSO treatment day 3 for both JG alone and Combination are indicated by * ($P<0.05$) and were assessed by the one-way ANOVA and Fisher's PLSD post-hoc.

CHAPTER 4 Discussions

The American Cancer Society estimates that in 2010 there will be over 1 million new cancer patients (American Cancer Society, 2010). These astronomical numbers also contribute to 1 in every 4 deaths, which equal about 1500 lives per day. Of those, colon cancer, breast cancer and melanoma are some of the most deadly malignancies when not detected early. The current microtubule targeting agents for metastatic disease are not very effective (Fojo et al., 2007; Sampath el al., 2006; Delaunoit et al., 2005). Even when the drugs are effective, they also have numerous debilitating toxicities. Cardiotoxicity, peripheral neuropathy and the development of drug resistance are a few of the major drawbacks associated with current cancer chemotherapy (American Cancer Society, 2009). Previous studies from our lab have shown the effects of JG-03-14 on MDA-MB-231, MCF-7 and MCF-7/E6 breast tumor cells, of which all appear to be sensitive to JG-03-14 through either apoptosis or autophagy (Arthur et al., 2007).

The primary findings of our studies are that both HCT-116 colon carcinoma cells and a B16F10 melanoma cell line are sensitive to the novel microtubule poison, JG-03-14. The initial response to treatment is cell death, primarily through autophagy. A residual surviving cell population is in a state of senescence, which appears to be irreversible, even when drug is removed as shown by the lack of proliferative recovery. Clonogenic survival studies indicate that at a concentration of 500 nM there is an approximate 98.5% reduction in

survival of HCT-116 cells and a 97.3% reduction in survival of the melanoma cells. The effects on clonogenic survival are markedly similar while the time course studies of cell killing demonstrate dramatic differences between the two cell lines. One hypothesis for the overall decreased sensitivity of the B16F10 cells is the high amount of what appears to be a basal autophagy, which has been mentioned by other groups (Tormo et al, 2009). This basal level of autophagy may stage the cells to enter into senescence at a more accelerated rate as opposed to entering autophagic cell death, similar to what has been reported in response to high concentrations of adriamycin (Vicencio et al., 2008; Di et al, 2006, 2009).

Cell Death by Autophagy

Autophagy is a process that involves the formation of double membrane acidic vesicles around cellular organelles such as mitochondrial or endoplasmic reticulum; the autophagosomes then fuse with lysosomes that provide the enzymes for degradation of the autophagolysosomal content (Dunn, 1994). In control acridine orange-stained cells, the cytoplasm and nucleus fluoresce bright green and dim red respectfully, whereas in cells undergoing autophagy, the acidic compartments fluoresce bright orange (Paglin et al., 2001). Our observations of autophagic vacuoles in JG-03-14 treated cells stained with acridine orange indicate the presence of autophagolysosomes. The untreated controls in both HCT and B16 cells generally show a single condensed large vacuole situated near the nucleus. The literature does indicate that in some

cases autophagy is an alternative mode of cell death when apoptosis is defective due to p53 mutations or its inhibition (Kim et al., 2006; Yu et al., 2006). However, since our cells are not p53 deficient, this explanation would not apply. Other work has shown that autophagy may contribute to the tumor suppressive function of p53, (Jin 2005; Zeng et al., 2007) and that p53 may be involved in the induction of autophagy (Tasdemir et al., 2008; Levine et al., 2008).

Autophagy was also confirmed using monodansylcadaverine staining in the both cell lines in response to JG-03-14. MDC is sometimes considered to be a more reliable indicator of autophagic vacuole formation because of its interaction with the autophagic membrane and not just the acidic compartment of the autophagosome (Biederbick et al., 1995). Transmission electron microscopy further substantiated the autophagic vesicle engulfing organelles and the autophagic machinery being executed in both the colon and melanoma cell lines.

A protein associated with autophagy is microtubule associated protein light chain 3. LC3-II is a proteolytic product of LC3-I that is required for the formation of autophagosomes and is a known marker of autophagy (Asanuma et al., 2003). Prior to the induction of autophagy, RFP-LC3 shows a diffuse localization of red within the cytoplasm, whereas once autophagy is induced, the cleaved protein will associate with the membrane of the autophagic vesicle. This punctuate pattern is indicative of the autophagic process (Zeng et al., 2007). Our RFP-LC3-II punctuate pattern within the cytoplasm further supports the conclusion of

autophagic activity after incubation with JG-03-14 in the HCT-116 cells (Niemann et al., 2000). We also attempted to transfect the B16F10 cells. The RFP-LC3 was successfully transferred and visualized, but we were not able to maintain the stability of the fluorescent protein. Consequently, we were unable to evaluate the stable expression model of the fluorescent protein in this cell line.

Autophagic Flux

Another protein that has provided experimental evidence for autophagy is p62/SQSTM1 (Moscat et al., 2009). P62 is a ubiquitous scaffold protein that is associated with membrane formation for autophagosomes. During autophagic flux, the double membrane vesicles will fuse with the lysosome and p62 will be degraded (Bjørkøy et al, 2009). Our studies demonstrate autophagic flux in the HCT-116 cells when treated with JG-03-14. Here again, the B16F10 cells did not show evidence of p62 protein expression across all treatments or controls, possibly due to the basal level of autophagy resulting in undetectable levels in our assays. We hope to use an odyssey bioluminescence assay in the future to amplify the protein expression and confirm if our prediction of autophagic flux is correct. In HCT-116 cells, we do show a decline in p62 levels after 48 hours of incubation with JG-03-14 as well as partial restoration when cells are treated concurrently with the lysomotropic inhibitor chloroquine.

Inhibition of Autophagy to validate a mode of cell death

In order to further confirm our findings that the primary mechanism of cell killing induced by JG-03-14 is autophagy; we utilized pharmacological agents to inhibit the autophagic process. Chloroquine and Bafilomycin A-1 are lysomotropic and H^+-ATPase inhibitors, respectively (Shintani et al., 2004; Yamamoto et al., 1998). These compounds have been shown to inhibit the fusion of the autophagosome and the lysosome, which in turn inhibits the last step of the autophagic process (Shintani et al., 2004). In our studies, we found that the inhibitors generated somewhat ambiguous outcomes. The combination of autophagic inhibitors with JG-03-14 seemed to have a partially protective response against cell killing. As the autophagic process was being inhibited, the final mechanism of cell death appeared to be converted to the apoptotic machinery. This blockade of autophagy could be visualized using MDC, acridine orange staining while apoptosis was detected by DAPI staining, and the TUNEL assay. The blockade to autophagy in HCT-116 cells was confirmed by restoration of p62 levels while apoptosis was confirmed by FACS analysis. These effects observed with JG-03-14 and the use of concurrent autophagic inhibitors redirecting the cell to apoptosis is similar to what others have reported with tamoxifen (Amaravardi et al., 2007).

Absence of apoptosis as the primary response to JG-03-14.

It was of particular interest that JG-03-14 failed to promote extensive apoptosis in either the HCT-116 cells or the B16F10 melanoma cells. This may

be related to the fact that both cell lines are wild type in p53 and previous work in MCF-7 cells demonstrated primarily autophagy induced by JG-03-14 in this p53 wild type cell line (Arthur et al., 2007). There appears to be an ambiguous role of p53 with regards to autophagy. A recent paper described how both the over expression and silencing of p53 can induce autophagy (Tasdemir et al., 2008). This may correlate to the dual role of autophagy being cytotoxic and cytoprotective (Baehrecke, 2005). The induction of p53 may also be cell protective if a DNA damaging agent activates the cell's DNA damage response to arrest the cells with intentions of DNA repair and proliferation (Tasdemir et al., 2008). p53 induction could also be a mechanism whereby the cell has endured DNA damage and is poised to undergo intrinsic apoptosis as a means of cellular suicide (Prabhudesai et al., 2007). With JG-03-14 treatments, we did not detect induction of p53. DAPI staining studies and cell cycle analyses indicated that both taxol and combretastatin A-4 are killing cells through a different mechanism. Taxol has been shown to induce G1 arrest and apoptosis whereas combretastatin A-4 may drive cells into the apoptotic pathway after being pre-staged by mitotic catastrophe (Wagenknecht et al., 1998; Blajeski et al., 2001; Vakifahmetoglu et al., 2008). Some microtubule poisons have shown similar arrest in G2/M, but are markedly different from JG-03-14 in that they can activate p53 to execute apoptosis (Sayed et al, 2001). Since the models tested with JG-03-14 all show minimal induction of apoptosis in a system that contains wild-type p53, this is consistent with the idea that another mode of cell death (autophagy)

is occurring. These findings could represent a unique advantage for the use of this drug in treatment of apoptosis resistant tumors.

Cell Cycle Arrest in Response to JG-03-14

In studies of drug effects on cell cycle distribution, we observed that the cells arrested primarily in the G2/M phase of the cell cycle. This is consistent with the effects of other microtubule depolymerizers (Azeddine et al., 1998; Quan et al., 2007). These observations suggest that JG-03-14 failed to activate the G1 cell cycle checkpoint; in fact, Western blotting indicated that JG-03-14 failed to induce either p53 or p21 (data not shown). Although other microtubule poisons have been shown to arrest cells in G2/M and conclude with promotion of apoptosis as a means for cell killing (Zhu et al, 2010), this was clearly not the case for JG-03-14. In JG-03-14 treated cells, autophagy does not appear to damage the nuclear contents based on DAPI staining, the TUNEL assay and non-induction of p53. We therefore believe the population of cells arrested in G2/M phase may show continual depolymerizing activity to destroy cellular contents until the possibility of recovery has been bypassed.

We also observed a hyperdiploid population after treatment of either B16F10 cells or HCT-116 cells with JG-03-14, likely due to the ability of cancer cells to undergo mitotic slippage out of the G2/M arrest and re-replicate their DNA in the absence of cytokinesis (Gross et al., 1995). However, this response was unexpected in these p53 wild type cells, since endoreduplication is generally associated with the absence of functional p53 to induce G1 arrest and to sustain

arrest in G2 (Aylon et al, 2006); functional p53 generally promotes arrest in G0/G1 to prevent post-mitotic slippage (Stewart et al., 1999; Elhajouji et al, 1998). In fact, our previous studies showed that MDA-MB-231 mutant p53 breast tumor cells, but not p53 wild type MCF-7 cells, undergo endoreduplication (Arthur et al, 2007). The ability of the wild type p53 HCT-116 colon cancer cells as well as the B16F10 melanoma cells to undergo mitotic slippage indicates that tumor cells can become polyploid even in cells with functional p53, presumably because checkpoint signaling downstream of p53 is attenuated.

Absence of mitotic catastrophe in response to JG-03-14

The fact that there was evidence of polyploidy indicated that the cells were attempting to undergo cytokinesis following the G2/M arrest. One possible outcome of aberrant mitosis would be mitotic catastrophe (Vakifahmetoglu et al., 2008). Cell death by mitotic catastrophe is characterized by the formation of nuclear envelopes around individual clusters of missegregated chromosomes. These are formed during the misguided or early entry into mitosis with aberrant cytokinesis. This then culminates with the accumulation of micronuclei and appears similar to necrotic cell death. Mitotic catastrophe remains to be fully defined biochemically but the mode of cell killing is also thought to be pre-stage to induction of apoptosis (Vakifahmetoglu et al., 2008). Caspase 3 and PARP cleavage as well as mitotic catastrophe have been seen in response to combretastatin (Vitale et al., 2006). Using Hoechst stain, we failed to detect evidence of mitotic catastrophe following treatment with JG-03-14.

Senescence and proliferative recovery

In our studies, we showed that not only did the JG-03-14 compound arrest the cells in the G2/M stage, but that JG-03-14 also produced a massive amount of cell killing within this same population of cells possibly following the arrest. After treatment, the cell population was monitored to determine if the surviving cells ultimately overcame the initial treatment and would regain proliferative capacity after the drug was removed. Our studies in both cell lines indicated that proliferative recovery was entirely disrupted. The cells were incapable of replication as far out as 17 days after replacement of drug medium with drug-free medium.

A large percent of the cells that were not killed entered into a senescent phase based on enlargement, flattening and lack of colony formation. Beta-galactosidase staining confirmed that this non-proliferating population was in fact senescent (Itahana et al., 2007; Arthur et al., 2007). Therefore, the variations in cell killing observed between the B16F10 cells and the HCT-116 may be due to the basal levels of autophagy (Tormo et al., 2009). The basal levels of autophagy in the B16F10 melanoma cells seen may pre-stage the melanoma cells to enter into senescence instead of massive amounts of autophagic cell death seen in the HCT-116.

Toxicity studies in cell culture and in vivo

Since microtubule poisons such as taxol and combretastatin have a number of undesirable dose limiting toxicities, including peripheral neuropathy

and cardiotoxicity among others (Scuteri et al., 2006; Stevenson et al., 2003), it was of importance to assess the influence of JG-03-14 on heart cells and to perform behavioral studies relating to neuropathy as an indication of its potential to cause neuropathic injury. In a preliminary dose response studies and using comparable doses of taxol and combretastatin, JG-03-14 appears to be least toxic of the three microtubule poisons. However, the relevance of this study to cardiac toxicity is somewhat questionable since the h9c2 cell line, unlike the heart, is a replicating model. Another microtubule poison, colchicine, is not used in the clinic because of associated peripheral neuropathy and being a substrate for the p-glycoprotein pump (Kuncl et al., 1987). This pump is one mechanism by which cancer cells can become resistant to chemotherapy and JG-03-14 has been shown not to be a substrate (Mooberry et al., 2007). Preliminary in vivo data also show there were no behavioral toxicity effects at doses of 100mg/kg and 200mg/kg. These findings together with studies indicating minimal toxicity in vivo suggest that JG-03-14 could be an improvement over the current clinical therapies.

Future Studies

Our studies have confronted a number of problems when using pharmacological inhibitors of autophagy. Chloroquine alone proved to be toxic in the B16F10 cells. Other autophagic inhibitors that target the PI3-K pathway such as Wortmannin, LY-249002 and 3-methyl adenine prove to be toxic at concentrations necessary to show autophagic inhibition. We therefore utilized

the late stage pharmacological inhibitors of autophagy at very low, non-toxic concentrations. An important study would be to use an inhibitor of caspase cleavage and possibly the induction of apoptosis. A pan-caspase inhibitor such as z-VAD in combination with JG-03-14 and a low dose autophagic inhibitor may divulge some mechanisms of cell response and possibly alter sensitivity (Yu et al., 2003). In order to fully understand the process, we also want to silence genes (atg's) as well as Beclin-1 (Suzuki et al., 2007; Yue et al., 2003). This approach would determine the reliance of JG-03-14 on autophagy proteins for cell killing. Since JG-03-14 has also been shown to induce apoptosis in other cell lines, the mechanism of cell killing may be cell type dependent (Arthur et al., 2007; Mooberry et al., 2007).

Knowledge of the precise signaling pathways for autophagic death induced by JG-03-14 remain to be defined, with a focus on mTOR and ER stress signaling. The literature suggests that autophagy could be a consequence of selective protein degradation, specifically catalase degradation causing an accumulation of ROS or degradation of other essential proteins that would eventually kill the cells (Yu et al., 2006; Onodera and Ohsumi, 2004). In concert with further defining the mechanism of action of JG-03-14, we would also like to see if it is as efficacious in vivo as it is in vitro. This would help define if the effects in cell culture are translational and could be applicable to the clinic. It would be of particular interest to test JG-03-14 in an immunocompetent mouse to see if some of the autophagic and senescent effects were to be cleared by the immune system.

Overview

In summary, these studies lead to a number of conclusions. Colchicine is not used in the clinic because it has been shown to be a substrate for the p-glycoprotein MDR pump as well as the glutathione S-transferase found in resistant cells (Ruiz-Gomez et al, 2000). Colchicine has also been shown to suppress bone marrow function (Liu et al, 2008; Harris et al, 2000) and to be highly toxic. In contrast, JG-03-14 had been determined not to be a substrate for the p-glycoprotein pump and to be relatively non-toxic (Mooberry et al, 2007).

Different microtubule targeting agents can cause either a G1 or G2 arrest, and the arrest may be p53-dependent or p53 independent. The fact that JG-03-14 induced a G2 arrest and there was no induction of p53 suggests that JG-03-14 may be less reliant on p53. This is significant in that cancers that acquire resistance via evasion of the p53-dependent mechanism may be sensitive to the alternative mechanism of cell cycle arrest that could ultimately lead to an alternative death signal. Since adjuvant radiotherapy is often used in preventing colon cancer recurrence, a G2/M block induced by JG-03-14 could stage the colon cancer cells for radiosensitization (Zheng, 2008; Jorgensen et al, 2007).

The results presented above have potentially important implications for JG-03-14 as a clinically effective agent due to its ability to promote autophagy.

By targeting autophagic induction of tumor regression, JG-03-14 may be able to bypass colon cancer and melanoma's high metastatic rate which typically accompanies resistance to apoptosis.

Drugs that target microtubules are important in cancer therapeutics, some of which are among the most effective in treating childhood and adult tumors. Though drugs such as combretastatin A-4 and 2ME2 bind to the same site on tubulin, they have different effects on tumor vasculature. 2ME2 has anti-angiogenic actions while combretastatin A-4 has anti-vascular activities that lead to a rapid collapse in tumor vasculature (Mooberry et al., 2003; Griggs et al., 2001). The ability of JG-03-14 to bind to tubulin and its action as a depolymerizer suggest its potential effects on tumor vasculature The maturation of angioblasts into endothelial cells is crucial for vascular tubule formation (Tozer et al, 1999). JG-03-14 at 100 nM concentration was able to inhibit endothelial cells tube formation, attachment, and migration, which indicates that JG-03-14 may have potential as a chemotherapeutic drug for cancer (Dalyot-Herman et al, 2009).

Literature Cited

Literature Cited

Alva, A.S., Gultekin, S.H., Baehrecke, E.H. (2004). Autophagy in human tumors: cell survival or death? *Cell Death and Differentiation.* 11, 1046–1048

Amaravadi, R.K., Duonan, Y., Lum, J.J, Thomas-Tikhonenko, A., and Thompson, C.B. (2007). Autophagy inhibition enhances therapy-induced apoptosis in a Myc-induced model of lymphoma. *Journal of Clinical Investigations.* 117(2), 326-336.

American Cancer Society.: Cancer Facts and Figures 2009. Atlanta, Ga: *American Cancer Society*, 2009.

Amundson, S. A., Myers, T. G., & Fornace, A. J.,Jr. (1998). Roles for p53 in growth arrest and apoptosis: Putting on the brakes after genotoxic stress. *Oncogene,* 17(25), 3287-3299.

Arthur, C. R., Gupton, J. T., Kellogg, G. E., Yeudall, W. A., Cabot, M. C., Newsham, I. F., et al. (2007). Autophagic cell death, polyploidy and senescence induced in breast tumor cells by the substituted pyrrole JG-03-14, a novel microtubule poison. *Biochemical Pharmacology,* 74(7), 981-991.

Asanuma, K., Tanida, I., Shirato, I., Ueno, T., Takahara, H., Nishitani, T., et al. (2003). MAP-LC3, a promising autophagosomal marker, is processed during the differentiation and recovery of podocytes from PAN nephrosis. *The FASEB Journal: Official Publication of the Federation of American Societies for Experimental Biology,* 17(9), 1165-1167.

Aylon, Y., Michael, D., Shmueli, A., Yabuta, N., Nojima, H., & Oren, M. (2006). A positive feedback loop between the p53 and Lats2 tumor suppressors prevents tetraploidization. *Genes & Development, 20*(19), 2687-2700.

Azad M.B., Chen Y., Henson E.S., Cizeau J., McMillan-Ward E., Israels S.J., Gibson S.B. (2008). Hypoxia induces autophagic cell death in apoptosis-competent cells through a mechanism involving BNIP3. *Autophagy.* 4(2):195-204.

Azeddine E, Cunha M, Kirsch-Volders M. Spindle poisons can induce polyploidy by mitotic slippage and micronucleate mononucleates in the cytokinesis-block assay. *Mutagenesis.* 1998;13:193–8.

Bajetta E, Del Vecchio M, Bernard-Marty C, Vitali M, Buzzoni R, Rixe O, Nova P, Aglione S, Taillibert S, Khayat D (2002). Metastatic melanoma: chemotherapy. *Seminars in Oncology.* 29 (5): 427–45

Bartek, J., & Lukas, J. (2001). Mammalian G1- and S-phase checkpoints in response to DNA damage. *Current Opinion in Cell Biology.* 13(6), 738-747.

Baunbaek, D., Trinkler, N., Ferandin, Y., Lozach, O., Ploypradith, P., Rucirawat, S., Ishibashi, F., Iwao, M., Meijer, L. (2008). Anticancer Alkaloid Lamellarins Inhibit Protein Kinases. *Marine Drugs.* 6(4): 514–527.

Biederbick, A., Kern, H. F., & Elsasser, H. P. (1995). Monodansylcadaverine (MDC) is a specific in vivo marker for autophagic vacuoles. *European Journal of Cell Biology, 66*(1), 3-14.

Bergers, G., & Benjamin L.E., (2003). Tumorigenesis and the angiogenic switch. Nature review.: *Cancer.* 3(6). 401-10.

Bjørkøy G., Lamark T., Pankiv S., Øvervatn A., Brech A., Johansen T. (2009). Monitoring autophagic degradation of p62/SQSTM1. *Methods of Enzymology.* 452, 181-197.

Blajeski, A. L., Phan, V. A., Kottke, T. J., & Kaufmann, S. H. (2002). G(1) and G(2) cell-cycle arrest following microtubule depolymerization in human breast cancer cells. *The Journal of Clinical Investigation,* 110(1), 91-99.

Boya, P., Gonzalez-Polo, R. A., Casares, N., Perfettini, J. L., Dessen, P., Larochette, N., et al. (2005). Inhibition of macroautophagy triggers apoptosis. *Molecular and Cellular Biology, 25*(3), 1025-1040.

Bright, S.A.,McElligott, A.M., O'Connell, J.W., O'Connor, L., Carroll, P., Campiani, G., Deininger, M.W., et al. (2010). Novel pyrrolo-1,5-benzoxazepine compounds display significant activity against resistant chronic myeloid leukaemia cells in vitro, in ex vivo patient samples and in vivo*. British Journal of Cancer.* 102, 1474-1482.

Campisi, J., (1997). The biology of replicative senescence. *Telomeres and Telomerase in Cancer.* 33(5), 703-709

Campisi, J., & d'Adda di Fagagna, F. (2007). Cellular senescence: when bad things happen to good cells. *Nature Reviews Molecular Cell Biology*. 8, 729-740.

Castedo, M., Perfettini, J., Roumier, T., Andreau, K., Medema R., and Kroemer, G. (2004) Cell death by mitotic catastrophe: a molecular definition. *Oncogene.* 23, 2825–2837.

Cazin, J.L., Gosselin, P., Cappelaere, P., Robert, J., & Demaille, A. (1992). Drug resistance in oncology: From concepts to applications. Journal *of Cancer Research and Clinical Oncology*, 119(2), 76-86.

Chin, L., Garraway, Levi A., Fisher, David E. (2006). Malignant melanoma: genetics and therapeutics in the genomic era. *Genes and Development*. 20 (16). 2149-82

Cui, Q., Tashiro, S., Onodera, S., Minami, M., & Ikejima, T. (2007). Oridonin induced autophagy in human cervical carcinoma HeLa cells through ras, JNK, and p38 regulation. *Journal of Pharmacological Sciences*, 105(4), 317-325.

Daylot-Herman, N., Delgago-Lopez, F., Gewirtz, D.A., Gupton, J.T., and Schwartz, E.L. (2009). Interference with endothelial cell function by JG-03-14, an agent that binds to the colchicine site on microtubules. *Biochemical Pharmacology.* 79(9). 1167-1177.

Deckbar, D., Stiff, T., Koch, B., Reis, C., Lobrich, M., and Jeggo P.A. (2010). The Limitations of the G1-S Checkpoint. *Cancer Research*. 70, 4412-4421

Delaunoit, T., Alberts, S. R., Sargent, D. J., Green, E., Goldberg, R. M., Krook, J., et al. (2005). Chemotherapy permits resection of metastatic colorectal cancer: Experience from intergroup N9741. *Annals of Oncology : Official Journal of the European Society for Medical Oncology / ESMO*, 16(3), 425-429.

Demasters, G., Di, X., Newsham, I., Shiu, R., & Gewirtz, D. A. (2006). Potentiation of radiation sensitivity in breast tumor cells by the vitamin D3 analogue, EB 1089, through promotion of autophagy and interference with proliferative recovery. *Molecular Cancer Therapeutics*, 5(11), 2786-2797.

Desai, A. & Mitchison, T.J. (1997). Microtubule polymerization dynamics. *Annual Review of Cell and Developmental Biology,* 13, 83-117.

Di Leonardo, A., Linke, S.P., Clarkin, K., Wahl, G.M. (1994) DNA damage triggers a prolonged p53-dependent G1 arrest and long-term induction of Cip1 in normal human fibroblasts. *Genes and Development*. 8, 2540-2551

Di, X., Shiu, R.P., Newsham, I.F., Gewirtz, D.A., (2009). Apoptosis, autophagy, accelerated senescence and reactive oxygen in the response of human breast tumor cells to adriamycin*. Biochemical Pharmacology*. 77(7):1139-50.

Druley, T.E., Stein, W.D., Ruth, A., Roninson, I.B. (2001). P-glycoprotein-mediated colchicine resistance in different cell lines correlates with the effects of colchicine on P-glycoprotein conformation*. Biochemistry*. 40(14), 4323-31.

Dunn Jr., W.A. (1994). Autophagy and related mechanisms of lysosome-mediated protein degradation. *Trends in Cell Biology.* 4(4), 139-143.

Eastman, A., & Schulte, N. (1988). Enhanced DNA repair as a mechanism of resistance to cisdiamminedichloroplatinum (II). *Biochemistry,* 27(13), 4730-4734.

Elhajouji, A., Cunha, M., & Kirsch-Volders, M. (1998). Spindle poisons can induce polyploidy by mitotic slippage and micronucleate mononucleates in the cytokinesis-block assay. *Mutagenesis, 13*(2), 193-198.

Elmore, L.W., Rehder, C.W., Di, X., McChesney, P.A., Jackson-Cook, C.K., and Gewirtz et al. (2002). Adriamycin-induced senescence in breast tumor cells involves functional p53 and telomere dysfunction. *Journal of Biological Chemistry*. 277, 35509-35515.

Elmore**,** L.W., Di,X., Di,Y-D, Holt,S.E., and Gewirtz,D.A.. 2005. Evasion of chemotherapy-induced senescence in breast cancer cell: implications for treatment response. *Clinical Cancer Research,* 2005 11(7):2637-43.

Erenpreisa J.E., Ivanov A., Dekena G., Vitina A., Krampe R., Freivalds T., Selivanova G., Roach H.I.(2000). Arrest in metaphase and anatomy of mitotic catastrophe: mild heat shock in two human osteosarcoma cell lines. *Cell Biology International*. 24(2), 61-70.

Fojo, A T., Ueda K., Slamon, D.J., Poplack, D.G. Gottesman, M.M., & Pastan, I. (1987). Expression of a multidrug-resistance gene in human tumors and

tissues. *Proceedings of the National Acedemy of Sciences of the United States of America*, 84(1), 265-269.

Fojo, T. & Menefee, M. (2007). Mechanisms of mulitdrug resistance: The potential role of microtubule-stabilizing agents. Annals of Oncology: *Official Journal of the European Society for Medical Oncology/ EMSO*, 18 Suppl 5, v3-8.

Gallegos-Arreola, M. P., Peralta-Leal, V., Morgan-Villela, G., & Puebla-Perez, A. M. (2008). Frequency of TS1494del6 polymorphism in colorectal patients from west of mexico.] *Revista De Investigacion Clinica; Organo Del Hospital De Enfermedades De La Nutricion*, 60(1), 21-30.

Gewirtz, D.A., Holt, S., Elmore, L. (2008). Accelerated senescence: An emerging role in tumor cell response to chemotherapy and radiation. *Biochemical Pharmacology.* 76(8). 947-957.

Gewirtz, D.A. (2009). Autophagy, senescence and tumor dormancy in cancer therapy*. Autophagy*. 5(8):1232-4.

Gewirtz, D.A. and Elmore, L.W. 2005. Apoptosis as a predominant tumor cell response to chemotherapy and irradiation: A case of TUNEL vision? *Current. Opinion of Investational Drugs,* 6(12):1199.

Gisselsson D. (2001) Chromosomal Instability in Cancer: Causes and Consequences. *Atlas of Genetics and Cytogenetics in Oncology and Haematology.*
< http://AtlasGeneticsOncology.org/Deep/ChromosomInstabilID20023.html >

Gozuacik, D., & Kimchi, A. (2004). Autophagy as a cell death and tumor suppressor mechanism. *Oncogene,* 23(16), 2891-2906

Gray-Schopfer, V., Wellbrock, C., Marais, R. (2007). Melanoma biology and new targeted therapy. *Nature.* 445(7130). 851-7.

Griggs, J., Metcalfe, J., Hesketh, R. (2001) Targeting tumour vasculature: the development of combretastatin A-4. *Oncology.* 2(2), 82-87

Gulbins, E. Jekle, A., Ferlinz, K. Grassme, H., & Lang, F. (2000). Physiology of apoptosis. *American Journal of Physiology. Renal Physiology*, 279(4), F605-15.

Hanahan D., Weinberg RA. The hallmarks of cancer. *Cell*. 2000;100:57-70.

Hancock BW, Wheatley K, Harris S, et al.(2004). Adjuvant interferon in high-risk melanoma: the AIM HIGH Study--United Kingdom Coordinating Committee on Cancer Research randomized study of adjuvant low-dose extended-

duration interferon Alfa-2a in high-risk resected malignant melanoma. *Journal of Clinical Oncology.* 22 (1): 53-61.

Harris, R., Marx, G., Gillett, M., Kark, A., & Arunanthy, S. (2000). COlchicine-induced bone marrow suppression: Treatment with granulocyte colony-stimulating factor. *The Journal of Emergency Medicine*. 18(4), 435-440.

Igbal, S. & Lenz, H.J. (2004). Angiogenesis inhibitors in the treatment of colorectal cancer. *Seminar in Oncology*, 31(6 Suppl 17), 10-16.

Iguchi, K., Usui, S., Ishida, R., Hirano, K. (2002) Imidazole-induced cell death, associated with intracellular acidification, caspase-3 activation, DFF-45 cleavage, but not oligonucleosomal DNA fragmentation . *Apoptosis.* 7(6) 1360-8185.

Itahana, K., Campisi, J., Dimri, G.P. (2007). Methods to Detect biomarkers of cellular senescence: the senescence-associated beta-galactosidase assay. *Methods of Molecular Biology.* 371, 21-31.

Ivanov, G.S., Ivanova, T., Kurash, J., Ivanov, A. et al. (2007). Methylation-Acetylation Interplay Activates p53 in Response to DNA Damage. *Molecular Cell Biology.* 27: 6756-6769.

Jin, S. (2005). p53, autophagy and tumor suppression. *Autophagy, 1*(3), 171-173.

Jones, K.R., Elmore, L.W., Jackson-Cook, C., Demasters, G., Povirk, L.F., Holt, S.E., Gewirtz, D.A. (2005). P53-Dependent accelerated senescence induced by ionizing radiation in breast tumour cells. *International Journal of Radiation Biology.* 81(6). 445-458.

Jones,K.R., Elmore, L.W.**,** Povirk,L., Holt,S.E., and Gewirtz,D.A.. (2005). Reciprocal regulation of senescence and apoptosis in response to radiation in the breast tumor cell. *International Journal of Radiation Biology*. 81(6):445-458.

Jusélius, J. & Sundholm, D., (2000). The aromatic pathways of porphins, chlorins and bacteriochlorins. *Physical Chemistry Chemical Physics*. 2: 2145–2151

Jordan, M.A., & Wilson, L., (1998). Microtubules and actin filaments: dynamic targets for cancer chemotherapy. *Current Opinion in Cell Biology*. 10(1), 123-130.

Jorgersen, T.J., Tian, H., Joesph, I.B., Menon, K., & Frost, D. (2007). Chemosensitization and radiosensitization of human lung and colon cancers by anti- mitotic agent, ABT-751, in athymic murine xenograft models of

subcutaneous tumor growth. *Cancer Chemotherapy and Pharmacology.* 59(6), 725-732.

Kabeya, Y., Mizushima, N., Ueno, T., Yamamoto, A., Kirisako, T., Noda, T., et al. (2000). LC3, a mammalian homologue of yeast Apg8p, is localized in autophagosome membranes after processing. *The EMBO Journal, 19*(21), 5720-5728.

Kaplan, R. N., Riba, R.D., Zacharoulis, S., Bramley, A.H. et al., (2005). VEGFR1-positive haematopoietic bone marrow progenitors initiate the pre-metastatic niche. *Nature*.430, 820-827.

Kim, K. W., Mutter, R. W., Cao, C., Albert, J. M., Freeman, M., Hallahan, D. E., et al. (2006). Autophagy for cancer therapy through inhibition of pro-apoptotic proteins and mammalian target of rapamycin signaling. *The Journal of Biological Chemistry, 281*(48), 36883-36890.

Kim, H.K., Park, S.K., Zhou, J., Taglialatela, G., Chung, K., Coggeshall, R.E., Chung, J.M. (2004). Reactive oxygen species (ROS) play an important role in a rat model of neuropathic pain. *Journal of the International Association for the Study of Pain.* 111(1). 116-124.

Kuncl, R.W., Duncan, G., Watson, D., Alderson, K., Rogawski, M.A., Peper, M. Colchicine myopathy and neuropathy. *New England Journal of Medicine.* 316(25), 1562-1568.

Kuo, C. C., Hsieh, H. P., Pan, W. Y., Chen, C. P., Liou, J. P., Lee, S. J., et al. (2004). BPR0L075, a novel synthetic indole compound with antimitotic activity in human cancer cells, exerts effective antitumoral activity in vivo. *Cancer Research*, 64(13), 4621-4628.

Lai, G.M., Ozols, R. F., Smyth, J.F., Young, R.C., & Hamilton, T.C. (1988). Enhanced DNA repair and resistance to cisplatin in human ovarian cancer. *Biochemical Pharmacology*, 37(24), 4597-4600.

Levine, B., & Abrams, J. (2008). p53: The Janus of autophagy? *Nature Cell Biology.* 10, 637 – 639.

Linos, E., Swetter, S. M., Cockburn, M. G., Colditz, G. A., Clarke, C. A. (2009). Increasing burden of melanoma in the United States. *The Journal of Investigative Dermatology.* 129 (7). 1666-74

Liu, W.C., Chuang, W.L., Tsai, M.L., Hong, J.H., McBride, W.H., & Chiang, C.S. (2008). Cordyceps sinensis health supplement enhances recovery from taxol induced leucopenia. *Experimental Biology and Medicine*. 233(4), 447-455.

Mathew, R., Karp, C.M., Beaudoin, B., Vuong, N., Chen, H.Y., Bray, K., Reddy, A., Bhanot, G., Geliana, C., Diapaola, R.S., Karantza-Wadsworth, V., White, E. (2009). Autophagy suppresses tumorigenesis through elimination of p62. *Cell.* 137(6), 1062-75.

Meschini, S., Condello, M., Calcabrini, A., Marra, M., Formisano, G., Lista, P., De Milito, A., Federici, E. and Arancia, G. (2008). The plant alkaloid voacamine induces apoptosis-independent autophagic cell death on both sensitive and multidrug resistant human osteosarcoma cells. *Autophagy* 4, 1020-1033.

Mignotte, B., & Vayssiere, J. (1998). Mitochondria and apoptosis. *European Journal of Biochemistry.* 252 (1), 1-15.

Mooberry, S.L., Mechanism of action of 2-methoxyestradiol: new developments. *Drug Resistance Updates.* 6(6), 355-361.

Mooberry, S. L., Weiderhold, K. N., Dakshanamurthy, S., Hamel, E., Banner, E. J., Kharlamova, A., et al. (2007). Identification and characterization of a new tubulin-binding tetrasubstituted brominated pyrrole*. Molecular Pharmacology*, 72(1), 132-140.

Moon, D., Kim, M., Kang, S., Lee, K., Heo, M., Choi, K., Choi, Y.H., Kim, G. (2008). Induction of G2/M arrest, endoreduplication, and apoptosis by actin

depolymerization agent pextenotoxin-2 in human leukemia cells, involving activation of ERK and JNK. *Biochemical Pharmacology*. 76(3). 312-321.

Mori, S., Sawada, T., Okada, T., Ohsawa, T., Adachi, M., & Keiichi, K. (2007). New anti-proliferative agent, MK615, from Japanese apricot "prunus mume" induces striking autophagy in colon cancer cells in vitro. *World Journal of Gastroenterology.* WJG, 13(48), 6512-6517.

Moscat, J., and Diaz-Meco, M.T. (2009) p62 at the Crossroads of Autophagy, Apoptosis, and Cancer. *Cell.* 137(6).

Mosmann, T. (1983). Rapid Colorimetric Assay for Cellular Growth and Survival: Application to Proliferation and Cytotoxicity Assays. *Journal of Immunological Methods.* 65, 55-63.

Moss, D.K., Betin, V.M., Malensinski, S.M., Lane, J.D. (2006). *Journal of Cell Science*. 119, 2362-2374

Nguyen, T., (2008). Promotion of Cell Death Through the Induction of Autophagy In HCT-116 Cancer Cells by Microtubule Poison, JG-03-14. *Master's Thesis – Virginia Commonwealth University, School of Medicine.*

Niemann, A., Baltes, J., & Elsasser, H. P. (2001). Fluorescence properties and staining behavior of monodansylpentane, a structural homologue of the

lysosomotropic agent monodansylcadaverine. *The Journal of Histochemistry and Cytochemistry : Official Journal of the Histochemistry Society, 49*(2), 177-185.

Niemann, A., Takatsuki, A., & Elsasser, H. P. (2000). The lysosomotropic agent monodansylcadaverine also acts as a solvent polarity probe. *The Journal of Histochemistry and Cytochemistry : Official Journal of the Histochemistry Society, 48*(2), 251-258.

Nogales, E. (2001) Structural insight into microtubule function. *Annual Review of Biophysics and Biomolecular Structure*, 30, 397-420.

Paglin, S., Hollister, T., Delohery, T., Hackett, N., McMahill, M., Sphicas, E., et al. (2001). A novel response of cancer cells to radiation involves autophagy and formation of acidic vesicles. *Cancer Research, 61*(2), 439-444.

Pasquier, E., & Kavallaris, M. (2008). Microtubules: A dynamic target in cancer therapy*. IUBMB Life,* 60(3), 165-170.

Prabhudesai, S.G., Rekhraj, S., Roberts, G., Darzi, A.W., Ziprin, P. (2007). Apoptosis and chemo-resistance in colorectal cancer. *Journal of Surgical Oncology.* 96(1), 77-88.

Ravikumar, B., Berger, Z., Vacher, C., O'Kane, C., and Rubinsztein, D.C. (2006). Rapamycin pre-treatment protects against apoptosis. *Human Molecular Genetics.* 15(7):1209-1216.

Roth, W., Wagenknecht, B., Grimmel, C., Dichgans, J., & Weller, M. (1998). Taxol-mediated augmentation of CD95 ligand-induced apoptosis of human malignant glioma cells: Association with bcl-2 phosphorylation but neither activation of p53 nor G2/M cell cycle arrest. *British Journal of Cancer*, 77(3), 404-411.

Ruiz Gomez, M. J., Gil, L., Souviron, A., & Martinez Morillo, M. (2000). Multidrug resistance increment in a human colon carcinoma cell line by colchicine. *Journal of Physiology and Biochemistry,* 56(1), 33-38.

Ruiz-Gomez, M. J., Souviron, A., Martinez-Morillo, M., & Gil, L. (2000). P-glycoprotein, glutathione and glutathione S-transferase increase in a colon carcinoma cell line by colchicine. *Journal of Physiology and Biochemistry,* 56(4), 307-312.

Sampath, D., Greenberger, L. M., Beyer, C., Hari, M., Liu, H., Baxter, M., et al. (2006). Preclinical pharmacologic evaluation of MST-997, an orally active taxane with superior in vitro and in vivo efficacy in paclitaxel- and docetaxel-

resistant tumor models. *Clinical Cancer Research : An Official Journal of the American Association for Cancer Research, 12*(11 Pt 1), 3459-3469.

Sayed, M., Pelech, S., Wong, C., Marotta, A., Salh, B., (2001). Protein kinase CK2 is involved in G2 arrest and apoptosis following spindle damage in epithelial cells. *Oncogene.* 20(48), 6994-7005.

Schwartz, R. N. (2008). Management of early and advanced colorectal cancer: Therapeutic issues. *American Journal of Health-System Pharmacy : AJHP : Official Journal of the American Society of Health-System Pharmacists,* 65(11 Suppl 4), S8-14.

Scorrano, L., Korsmeyer, S.J. (2003). Mechanisms of cytochrome c release by proapoptotic BCL-2 family members. *Biochemical and Biophysical Research Communications.* 304 (3), 437-444.

Scuteri, A., Nicolini, G., Miloso, M., Bossi, M., Cavaletti, G., Windebank, A.J., and Tredici, G. (2006). Paclitaxel toxicity in post-mitotic dorsal root ganglion (DRG) cells. *Anticancer Research*. 26(2A), 1065-1070.

Seglen, P.O., & Gordon, P.B., (1982). 3-methyladenine: Specific inhibitor of autophagic/lysosomal protein degradation in isolated rat hepatocytes. *Proceedings of the National Acedemy of Sciences of the United States of America.*79(6), 1889-1892.

Shacka, J. J., Klocke, B. J., & Roth, K. A. (2006). Autophagy, bafilomycin and cell death: The "a-B-cs" of plecomacrolide-induced neuroprotection. *Autophagy, 2*(3), 228-230.

Shacka, J. J., Klocke, B. J., Shibata, M., Uchiyama, Y., Datta, G., Schmidt, R. E., et al. (2006). Bafilomycin A1 inhibits chloroquine-induced death of cerebellar granule neurons. *Molecular Pharmacology, 69*(4), 1125-1136.

Shellman Y.G., Park Y. L., Marr, D.G., Casper, K., Xu, Y., Fujita, M., Swerlick, R., Norris, D.A., (2003). Release of vascular endothelial growth factor from a human melanoma cell line, WM35, is induced by hypoxia but not ultraviolet radiation and is potentiated by activated Ras mutation. *Journal of Investigative Dermatology.* 121(4):910-7.

Shen, Y., & White, E. (2001). p53-dependent apoptosis pathways. *Advanced Cancer Research.* 82:55-84

Shia, J. (2008). Immunohistochemistry versus microsatellite instability testing for screening colorectal cancer patients at risk for hereditary nonpolyposis colorectal cancer syndrome. Part I. The utility of immunohistochemistry. *The Journal of Molecular Diagnostics: JMD*, 10 (4), 293-300.

Shintani, T., & Klionsky, D. J. (2004). Autophagy in health and disease: A double-edged sword. *Science (New York, N.Y.), 306*(5698), 990-995.

Shao, Y., Gao, Z., Marks, P.A., Jiang, X. (2004). Apoptotic and autophagic cell death induced by histone deacetylase inhibitors. *Proceedings of the National Academy of Sciences.* 101(52), 18030-18035.

Sliwinska, M.A., Mosieniak, G., Wolanin, K., Babik, A., Piwocka, K.,et al. (2009). Induction of senescence with doxorubicin leads to increased genomic instability of HCT-116. *Mechanisms of Ageing and Development.* 130(1-2), 24-32.

Stewart, Z. A., Mays, D., & Pietenpol, J. A. (1999). Defective G1-S cell cycle checkpoint function sensitizes cells to microtubule inhibitor-induced apoptosis. *Cancer Research, 59*(15), 3831-3837.

Stewart, Z. A., & Pietenpol, J. A. (1999). Cell cycle checkpoints as therapeutic targets. *Journal of Mammary Gland Biology and Neoplasia, 4*(4), 389-400.

Stevenson, J.P., Rosen, M., Sun, W., Gallagher, M., et al. Phase I Trial of the Antivascular Agent Combretastatin A4 Phosphate on a 5-Day Schedule to Patients With Cancer: Magnetic Resonance Imaging Evidence for Altered Tumor Blood Flow. *Journal of Clinical Oncology.* 21(23), 4428-4438.

Sudo, T., Nitta, M., Saya, H. & Ueno, N.T. (2004) Dependence of paclitaxel sensitivity on a functional spindle assembly checkpoint. *Cancer Research.* 64(7), 2502-2508.

Suzuki, K., Kubota, Y., Sekito, T., Ohsumi, Y. (2007). Hierarchy of Atg proteins in the pre-autophagosomal structure organization. *Genes to Cells.* 12, 209-218.

Tasdemir, E., Maiuri, M.C., Galluzzi, L., Vitale, I., Djavaheri-Mergny, M. et al. (2008). Regulation of autophagy by cytoplasmic p53. *Nature Cell Biology.* 10(6), 676-87.

Taylor, R. C., Cullen, S. P., & Martin, S. J. (2008). Apoptosis: Controlled demolition at the cellular level. *Nature Reviews.Molecular Cell Biology*, 9(3), 231-241.

Thorburn, J., Horita, H., Redzic, J., Hansen, K., Frankel, A.E., Thorburn, A. (2009) Autophagy regulates selective HMGB1 release in tumor cells that are destined to die. *Cell Death and Differentiation*. 16(1): 175–183.

Tormo, D., Checinska, A., Alonso-Curbelo, D., Perez-Guijarro, E., Canon, E., Riveiero-Falkenbach, E., Calvo, T.G., Larriebere, L., Megais, D., Mulero, F. et al. (2009). Targeted activation of innate immunity for therapeutic induction of autophagy and apoptosis in melanoma cells. *Cancer Cell.* 16(2), 103-14.

Tozer, G.M., Prise, V.E., Wilson, J., Locke, R.J., Vojnovic, B., Stratford, M.R., et al. (1999). Combretastatin A-4 phosphate as a tumor vascular-targeting agent: Early effects in tumors and normal tissues. *Cancer Research.* 59(7), 1626-1634.

Tsao H., Cosimi A.B., Sober A.J., (1997). Ultra-late recurrence (15 years or longer) of cutaneous melanoma. *Cancer* 79 (12): 2361-70.

Twiddy, D., Cain, K. (2007). Caspase-9 cleavage, do you need it? *Biochemical Journal*. 405(Pt 1), e1.

Vakifahmetoglu, H., Olsson, M., & Zhivotovsky, B. (2008). Death through a tragedy: Mitotic catastrophe. *Cell Death and Differentiation*, 15(7), 1153-1162.

Vicencio J.M., Galluzzi L., Tajeddine N., Ortiz C., Criollo A., Tasdemir E., Morselli E., Ben Younes A., Maiuri M.C., Lavandero S., Kroemer G. (2008). Senescence, apoptosis or autophagy? When a damaged cell must decide its path--a mini-review. *Gerontology.* 54(2):92-9.

Vitale, I., Antoccia, A., Cenciarelli, C., Crateri, P., Meschini, S., Arancia, G., Pisano, C., and Tanzarella, C. (2007). Combretastatin CA-4 and combretastatin derivative induce mitotic catastrophe dependent on spindle checkpoint and caspase-3 activation in non-small cell lung cancer cells. *Apoptosis.* 12(1), 155-166.

Vivanco, I., & Sawyers, C. L. (2002). The phosphatidylinositol 3-kinase AKT pathway in human cancer. *Nature Reviews.Cancer, 2*(7), 489-501.

Wagenknecht, B., Schulz, J.B., Gulbins, E., Weller, M. (1998). *Cell Death and Differentiation.* 5(10), 894-900.

Wattel E., Preudhomme C., Hecquet B., Vanrumbeke M., Quesnel B., Dervite I., Morel P., Fenaux P. (1994). p53 mutations are associated with resistance to chemotherapy and short survival in hematologic malignancies*. Blood.* 84(9), 31 48-57.

Weaver, B. A., & Cleveland, D. W. (2005). Decoding the links between mitosis, cancer, and chemotherapy: The mitotic checkpoint, adaptation, and cell death. *Cancer Cell,* 8(1), 7-12.

Xiao Z., Xue J., Semizarov D., Sowin T.J., Rosenberg S.H., Zhang H. (2005). Novel indication for cancer therapy: Chk1 inhibition sensitizes tumor cells to antimitotics*. International Journal of Cancer*. 115(4):528-38.

Xu, F.L., Rbaibi, Y., Kiselyov, K., Lazo, J., Wipf, P., and Saunders, W.S. (2010). Mitotic slippage in non-cancer cells induced by a microtubule disruptor, disorazole C1*. BMC Chemical Biology*. 10: 1.

Xue, W., Zender, L. Miething, C., Dickins, R.A., Hernando, E., Krizhanovsky, V., Cordon-Cardo, C., and Lowe, S.W. (2007). Senescence and tumour clearance is triggered by p53 restoration in murine liver carcinomas. *Nature.* 445, 656-660.

Yamamoto, A., Tagawa, Y., Yoshimori, T., Moriyama, Y., Masaki, R., & Tashiro, Y. (1998). Bafilomycin A1 prevents maturation of autophagic vacuoles by inhibiting fusion between autophagosomes and lysosomes in rat hepatoma cell line, H-4-II-E cells. *Cell Structure and Function, 23*(1), 33-42.

Ylä-Anttila P., Vihinen H., Jokitalo E., Eskelinen E.L. (2009). Monitoring autophagy by electron microscopy in Mammalian cells. *Methods of Enzymology.* 452, 143-64.

Young, A. R., Narita, M. (2010). Connecting autophagy to senescence in pathophysiology. *Current Opinion in Cell Biology, Cell Regulation.* 22(2), 234-240

Young, A.R., Narita, Ferrerira, M., Kirschner, K., Sadaie, M., Darot, J.F.J, Tavaré S., et al. (2009). Autophagy mediates the mitotic senescence transition. *Genes & Development*. 23: 798-803

Yu, L., Wan, F., Dutta, S., Welsh, S., Liu, Z., Freundt, E., et al. (2006). Autophagic programmed cell death by selective catalase degradation. *Proceedings of the National Academy of Sciences of the United States of America, 103*(13), 4952-4957.

Yue, Z., Jin, S., Yang, C., Levine, A.J., Heintz, N., Beclin 1, an autophagy gene essential for early embryonic development, is a haploinsufficient tumor

suppressor. *Proceedings for the National Academy of Sciences.* 100(25), 15077-15082.

Zeng, X., Yan, T., Schupp, J. E., Seo, Y., & Kinsella, T. J. (2007). DNA mismatch repair initiates 6-thioguanine--induced autophagy through p53 activation in human tumor cells. *Clinical Cancer Research : An Official Journal of the American Association for Cancer Research, 13*(4), 1315-1321.

Zhai, Y., Kronebusch, P.J., Simon, P.M., Borisy, G.G. (1996). Microtubule dynamics at the G2/M transition: abrupt breakdown of cytoplasmic microtubules at nuclear envelope breakdown and implications for spindle morphogenesis. *The Journal of Cell Biology*. 135(1). 201-214.

Zhou, M., Gu, L., Findley, H.W., Jiang, R., and Woods, W.G. (2003). PTEN Reverses MDM2-mediated Chemotherapy Resistance by Interacting with p53 in Acute Lymphoblastic Leukemia Cells. *Cancer Research.* 63, 6357-6362.

Zhu, H., Zhang, J., Xue, N., Hu, Y., Yang, B., He, Q. et al. (2010). Novel combretastatin A-4 derivative XN0502 induces cell cycle arrest and apoptosis in A549 cells. *Investigational New Drugs.* 28(4), 493-501.

Zordoki, B.N.M., & El-Kadi, A.O.E. (2007). H9c2 cell line is a valuable in vitro model to study the drug metabolizing enzymes in the heart. *Journal of Pharmacological and Toxicological Methods*. 56(3), 317-322.

Zrieki, A., Farinotti, R., & Buyse, M. (2008). Cyclooxygenase inhibitors down regulate P-glycoprotein in human colorectal caco-2 cell line. *Pharmaceutical Research*, 25(9):1991-2001.

VITA

Jonathan W. Biggers is 24 years old and was born in Bloomington, Illinois on July 15th, 1985. He earned his Bachelor's of Science in Human Nutrition of Foods and Exercise from Virginia Tech University in 2007 and joined Dr. Gewirtz lab in 2008. He will be continuing his education at Edward Via College of Osteopathic Medicine in the Fall of 2010.